JACS
JOURNAL OF THE AMERICAN CHEMICAL SOCIETY

Perspective

pubs.acs.org/JACS

Integrated Materials Design of Organic Semiconductors for Field-Effect Transistors

Jianguo Mei, Ying Diao, Anthony L. Appleton, Lei Fang, and Zhenan Bao*

Department of Chemical Engineering, Stanford University, Stanford, California 94305, United States

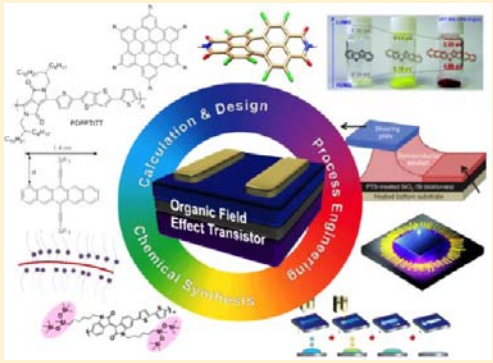

ABSTRACT: The past couple of years have witnessed a remarkable burst in the development of organic field-effect transistors (OFETs), with a number of organic semiconductors surpassing the benchmark mobility of 10 $cm^2/(V\ s)$. In this perspective, we highlight some of the major milestones along the way to provide a historical view of OFET development, introduce the integrated molecular design concepts and process engineering approaches that lead to the current success, and identify the challenges ahead to make OFETs applicable in real applications.

1. INTRODUCTION

A field-effect transistor (FET) is an electronic device that amplifies and switches electrical signals. The development of metal−oxide−semiconductor field-effect transistors (MOSFETs) and integrated circuits (microprocessors) has forever changed our everyday lives since their inventions more than 50 years ago. Today, we are facing a new technological evolution that could possibly have a similar impact on our lives—the emergence of flexible and printed electronics. Among them, organic field-effect transistors (OFETs) have been conceptualized and developed over the past two decades.[1,2] Currently, the performance of OFETs is surpassing that of amorphous silicon (*a*-Si) FETs with field-effect mobilities of 0.1−1 $cm^2/(V\ s)$ and on/off ratios of 10^6−10^8, and is approaching that of poly crystalline silicon (*c*-Si) FETs (>10 $cm^2/(V\ s)$). The state-of-the-art charge carrier mobilities for thin film OFETs are 17.2 $cm^2/(V\ s)$ in the case of vacuum-deposited small molecules,[3] 31.3 $cm^2/(V\ s)$ for solution-processed small molecules,[4] and 10.5 $cm^2/(V\ s)$ for conjugated polymers.[5] For bulk single crystal devices, mobility as high as 15−40 $cm^2/(V\ s)$ has been reported.[6−9] Accordingly, OFETs are being considered for applications in radio frequency identification tags (RFIDs), electronic paper, organic light emitting displays, sensor devices and beyond.

1.1. A Brief Overview of Organic Field-Effect Transistors.

OFETs were first fabricated using electrochemically polymerized conjugated polymers[10] and subsequently small molecules in the 1980s.[11] Initially, these devices were merely considered to be an experimental tool to characterize the charge transport properties of organic semiconductors (OSCs), as it was difficult to measure electrical properties of undoped organic solids. In those days, OFETs exhibited rather low charge mobility (several orders of magnitude lower than *a*-Si FETs) with poor storage and operation stability, far from meeting the requirements for any realistic applications. Nevertheless, the concept of printed electronics was first demonstrated with OFETs in the 1990s with the development of solution processable organic semiconductors,[12−17] which sparked the demonstration of various other printed electronic and optical components.[18−22] The past few years have witnessed significant progress in the performance of OFETs. Here, we highlight some of the major milestones in the course of OFET development.

Vacuum-deposited OFETs (VD-OFETs) have been extensively investigated. Various π-conjugated oligomers (e.g., oligothiophenes[23,24]) and marcocyclic compounds (e.g., copper phthalocyanines, CuPc[25]) were synthesized and tested.[26] Pentacene is one of the first OSCs that showed record mobility values initially greater than 0.1 $cm^2/(V\ s)$ on SiO_2/Si substrates,[27] subsequently reaching 1.5 $cm^2/(V\ s)$ on chemically modified SiO_2/Si substrates,[28] and then 3−6 $cm^2/(V\ s)$ on polymer gate dielectrics.[1,29−31] Later, when a pentacene quinone was used to modify the dielectric surface, a record mobility of 35 $cm^2/(V\ s)$ was reported.[32] Even though pentacene based OFETs have been incorporated into some prototype electronic devices,[33−35] their commercialization is still largely hindered because of the difficulty associated with pentacene purification, as well as poor device storage and operation stability. Therefore, a large number of small molecule organic semiconductors have been designed and prepared, leading to mobilities higher than 1.0 $cm^2/(V\ s)$ and ranging from linear acenes to tetrathiafulvalene derivatives, coronene derivatives and metal phthalocyanines.[2] Currently, the state-of-art VD-OFETs based on alkylated dinaphtho[2,3-*b*:2′,3′-*f*]thieno[3,2-*b*]thiophenes (C_n-DNTTs) have reached thin film mobility close to 8.0 $cm^2/(V\ s)$ and a high on/off ratio of 10^8, with good environmental storage stability.[36] Unfortunately, operation stability was not given in this study. Very recently, an asymmetric 2-tridecyl[1]benzothieno[3,2-*b*][1]-benzothiophene (C_{13}-BTBT) molecule gave a record mobility of 17.2 $cm^2/(V\ s)$. About 60% mobility loss, however, was

Received: January 26, 2013
Published: April 4, 2013

   dx.doi.org/10.1021/ja400881n | *J. Am. Chem. Soc.* 2013, 135, 6724−6746

observed after running for 13h under ambient conditions.[3] Encapsulation is therefore required for most VD-OFETs.[37,38]

Vacuum deposition is a useful technique to deposit OSC thin films for OFETs. However, this approach is not amenable to low-cost and fast production. Solution processing is of great interest because it is compatible with the widely used high-throughput printing techniques and can potentially lead to low-cost fabrication. In this regard, solution-processed OFETs (SP-OFETs) have received a great deal of attention. SP-OFETs can be divided into two categories based on the active materials, namely small molecule and polymer based SP-OFETs.

SP-OFETs based on soluble oligothiophenes, substituted acenes and alkylated marcocyclic compounds have been subjected to extensive investigation.[2,39−47] Other types of SP-OFETs are processed through soluble precursors, in which actual functional OSCs are generated in the later stage via thermal treatment or photoiradiation.[48−51] This method has been often used in linear acenes.[27,52,53] The performance of SP-OFETs and VD-OFETs based on the same molecule, however, can be drastically different. In other words, processing conditions play a critical role in charge transport properties. Currently, there are only a few solution-processable small molecule OSCs with charge mobilities over 1.0 $cm^2/(V\ s)$.[42,54,55] The most notable example is 6,13-bis(triisopropylsilylethynyl)pentacene (TIPS-PEN), which has recently displayed a mobility of 4.6 $cm^2/(V\ s)$ by tuning the molecular packing using a solution shearing (SS) process.[56] Benzothieno[3,2-*b*][1]benzothiophene (BTBT) derivatives constantly exhibit high mobilities in SP-OFETs.[54,57]

In the case of solution-processed polymer OFETs (SPP-OFETs), regioregular poly(3-hexylthiophene) (P3HT) was the first polymer semiconductor that displayed high charge carrier mobility.[13,58,59] However, P3HT suffers from poor environmental stability because of its relatively high oxidative potential. Subsequent tuning through reducing the number of side chains[60] and introducing fused ring systems (such as thieno[3,2-*b*]thiophene polymer, PBTTT)[61] improved both stability and mobility. Notably, PBTTT gave charge-carrier field-effect mobilities of 0.2−0.6 $cm^2/(V\ s)$ and on/off ratios of 10^6−10^7. More importantly, the performance of the polymers on exposure to low-humidity (∼4%) air showed good operational stability with almost unnoticeable change of mobility, together with only a small positive threshold voltage shift and a slight decrease in the on/off ratio. Unfortunately, these devices still could not survive in ambient conditions (humidity level ∼50%). Moving from PBTTT to tetrathienoacene copolymers[62] and naphthodithiophene-based polymers,[63] both performance and stability have been improved. More recently, donor−acceptor type polymers showed remarkable mobility, such as cyclopentadithiophene− benzothiadiazole,[64] diketopyrrolopyrrole[5,65,66] and isoindigo[67−69] based polymers. Charge-carrier mobility values of SPP-OFETs have been pushed into the regime of *c*-Si FETs.[5,67,70,71] Importantly, some of these OFETs can be operated under ambient conditions for a prolonged time.[68,69]

Single crystal organic field-effect transistors (SC-OFETs) usually exhibit high charge mobilities owing to a high degree of order, low impurity concentration and absence of grain boundaries.[72−80] For instance, rubrene-based SC-OFETs consistently exhibited mobilities higher than 10 $cm^2/(V\ s)$.[9,80−83] A SC-OFET is an excellent platform for charge transport studies and for understanding device physics. Due to their excellent performance, SC-OFETs have been explored in applications such as OFET-driven flexible active-matrix displays and sensor arrays.[83] However, precise patterning of single-crystals while controlling their crystal orientations at active channel regions has presented serious technical challenges. The typically required manual placement of crystals is not an option for any practical application. To take advantage of the excellent performance of organic single crystals as active materials in these devices, some approaches have shown promise to overcome these technical obstacles in a high throughput manner.[74,76,77,84,85]

Solution-processed single crystal organic field-effect transistors (SPSC-OFETs) represent a new paradigm that combines excellent charge transport properties and fast solution-processing capability. As an example, TIPS-PEN has been studied in VD-OFETs, SP-OFETs (polycrystalline) and SPSC-OFETs. The optimized charge mobilities of TIPS-PEN for VD-OFETs,[86] SP-OFETs[87] and SPSC-OFETs[56,88] are 0.4, 1.8, and 3.8 $cm^2/(V\ s)$, respectively. Recently, Hasegawa and co-workers have devised an inkjet printing technique to process 2,7-dioctyl[1]benzothieno[3,2-*b*][1]benzothiophene ($2C_8$-BTBT) and obtained a record mobility of 31.3 $cm^2/(V\ s)$ with an average mobility of 16.4 $cm^2/(V\ s)$ in SPSC-OFETs,[4] while polycrystalline SP-OFETs of $2C_8$-BTBT obtained via spin-coating only exhibited 1.80 $cm^2/(V\ s)$. More details will be given in section 3.2.

1.2. The Scope of the Perspective. To date, a wide variety of OSCs have shown mobilities of 0.1−1 $cm^2/(V\ s)$. Some of them are in the range of 1−10 $cm^2/(V\ s)$. A few of them have even broken the benchmark of 10 $cm^2/(V\ s)$.[3,5,89,90] There is no doubt that progress is the result of a successful combination of developments in materials design, processing, fabrication and device engineering. This perspective aims at summarizing the general strategies that have been proven effective in molecular design and process engineering of OSCs for thin-film transistors. It is not meant to be a comprehensive review on OFET materials, which is the subject of several recent reviews.[2,70,91−93] Since the electronic properties of organic solids are highly dependent on molecular packing, film morphology, and interfacial properties, we emphasize that an integrated materials design approach is crucial whereby molecular design, morphology and molecular packing control, and device level engineering are considered as a whole, rather than discretely. The scope of this perspective is illustrated in Figure 1.

We set off with a brief overview of OFETs to highlight some of the major milestones during their developments to provide a historical perspective. We then summarize important principles used for designing high performance small molecules and conjugated polymers. A brief discussion on a few unconventional strategies is also provided. Subsequently, we discuss the use of process engineering as a powerful tool to further control molecular packing and morphology to realize high performance OFETs. Finally, we outline rational design approaches, which is the ultimate goal for designing functional materials. In this part, we will review recent progress in computer-aided design of high performance organic semiconductors by *in silico* screening.

2. MOLECULAR DESIGN OF ORGANIC SEMICONDUCTORS: A CHEMICAL APPROACH

The rate of charge transport, according to Marcus theory, in OCSs absent of any defects is governed by electron−electron and electron−vibration (phonon) interactions, which can be characterized using transfer integral and reorganization energy,

dx.doi.org/10.1021/ja400881n | *J. Am. Chem. Soc.* 2013, 135, 6724−6746

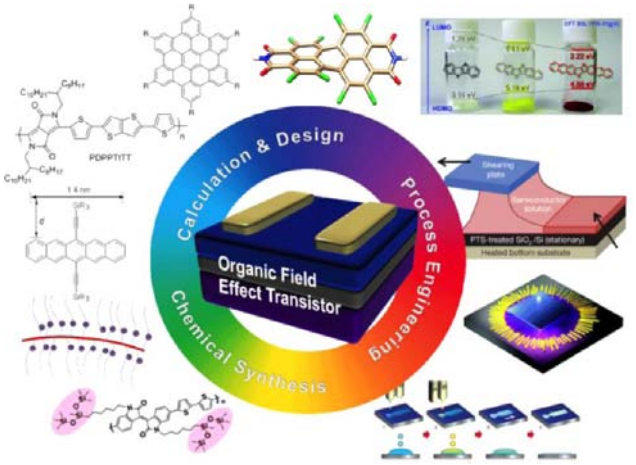

Figure 1. Illustration of the scope of this perspective.

respectively.[94−96] The transfer integral describes the degree of molecular orbital overlap of adjacent molecules, which is dependent on $\pi-\pi$ distance, orientation, and relative displacement distance. The reorganization energy in Marcus theory is defined as the energy required to "reorganize" the molecular structure from initial to final coordinates in order to accommodate charge transfer. Both transfer integral and reorganization energy are closely related to molecular structure, as well as molecular arrangements (packing) in the solid states. Generally speaking, a combination of large transfer integral and small reorganization energy leads to higher charge carrier mobility. However, many other factors can also have an impact, such as defects (disorders), impurities, charge carrier densities, electrical fields, temperature and pressure. It is nearly impossible to accurately predict the charge transport properties of small molecules or polymers from their individual molecular structures due to an inability to predict the extent of some of the aforementioned factors. However, some empirical molecular design rules have been found useful in designing promising OSCs. Our goal is to focus on some of the most successful examples to illustrate the role of molecular design on charge transport properties.

2.1. The Structures of Organic Semiconductors. A representative π-conjugated system is illustrated in Scheme 1.

Scheme 1. Illustration of a π-Conjugated System

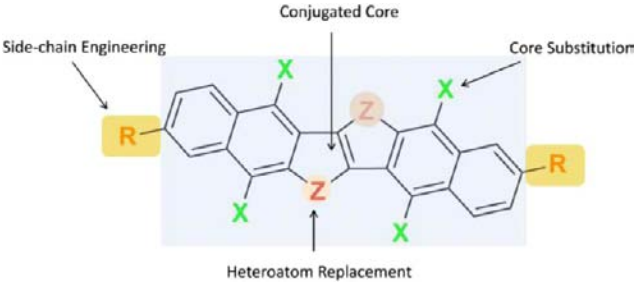

Such a structure can be a discrete molecule, a part of a conjugated oligomer or a repeat unit in a conjugated polymer. For the sake of discussion, we divide it into four constituting components: the conjugated core (backbone), heteroatoms, substituents (electron donating or withdrawing), and side chains (i.e., solubilizing groups). The conjugated core (backbone) determines most of the electronic properties (e.g., energy level and bandgap, inter/intramolecular interaction, and solubility) and influences molecular packing. Heteroatom replacement is an effective way to tune electronic properties, solubility and molecular packing. Core substitution also affects electronic properties, solubility and molecular arrangements, through modifying the dipole, changing the C/H ratio or halogen (chalcogen)−halogen (chalcogen) interactions. Side chains are usually incorporated to impart solubility, while they may also impact electronic properties in the solid state by changing molecular packing structures or altering the torsion conformation of the conjugated backbone. The side chains are typically insulating. Therefore, they lower the mass percentage of conjugated segments in the channel if excessive amounts of side chains are present. Below, we summarize the key design rules for each constituting component.

2.2. Conjugated Core: The Effect of Conjugation Extension and Aromaticity. Linear acenes are aromatic hydrocarbons composed of ladder-like fused benzene rings, as shown in Figure 2a. They have been of great interest both from a theoretical point of view and a performance perspective. Anthracene, the smallest member of the acene family with reported transistor characteristics, showed a mobility of 0.02 $cm^2/(V\ s)$ measured at low temperature in SC-OFETs.[97] Tetracene has one more ring than anthracene, therefore has a slightly longer conjugation length. SC-OFETs based on

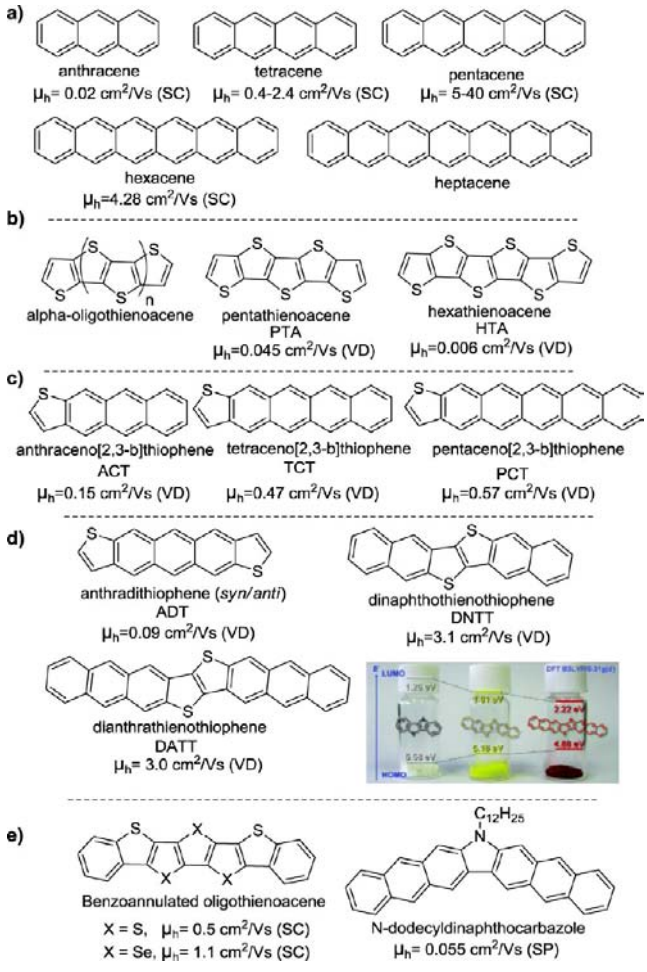

Figure 2. Representative acenes and heteroacenes. The inset in panel d was reproduced with permission from ref 112. Copyright 2011 American Chemical Society.

dx.doi.org/10.1021/ja400881n | J. Am. Chem. Soc. 2013, 135, 6724−6746

Table 1. Calculated Hole-Transporting Properties of Linear Acenes

acenes	HOMO[a] (eV)	λ^{+a} (meV)	R (Å), t^+ (meV)[b] T_1	T_2	P	L	μ^{+c} (cm^2/(V s))
Naphthalene	−5.80	183	5.01, 8	5.01, 8	5.93, 36	8.64, 0	0.0511
Anthracene	−5.24	138	5.22, 19	5.22, 19	6.01, 42	11.12, 0	0.158
Tetracene	−4.87	113	4.77, 70	5.13, 22	6.06, 37	13.44, 1	0.470
Pentacene	−4.61	95	4.76, 79	5.21, 45	6.27, 31	16.11, 1	0.832
Hexacene	−4.42	79	4.72, 88	5.22, 60	6.31, 37	18.61, 1	1.461

[a]B3LYP/6-31G(d,p) level. [b]PW91/DZ2P level calculated at 300 K (t^+ is given as absolute value) [c]Averaged value along the four directions (T_1, T_2, P and L) under consideration. Reproduced with permission from ref 101. Copyright 2012 Nature Publishing Group.

tetracene showed higher mobilities in the range of 0.4−2.4 cm^2/(V s).[81,98] Pentacene, one of the most studied acenes, has five linearly fused benzene rings exhibiting an even higher degree of conjugation. Charge mobilities for pentacene-based SC-OFETs are in the range of 5−40 cm^2/(V s).[7,99] Hexacene has also been successfully prepared through the photoinduced elimination of CO molecules from a diketone precursor.[100] Unfortunately, charge measurements were not available in this study. Very recently, a new synthetic approach through the CO elimination reaction from a monoketone precursor was used to prepare hexacene. Blue-green platelet-shaped hexacene crystals were obtained via a physical vapor-transport method. SC-OFETs based on hexacene exhibited mobility up to 4.28 cm^2/(V s), with an on/off ratio of 1×10^5.[101] In comparison, the hole mobility of pentacene-based SC-FETs fabricated in an identical manner was 1.2 cm^2/(V s) with an on/off ratio of 3×10^6. It was also observed that the conductivity of a hexacene single crystal measured under gate-free conditions was estimated to be 2.21×10^{-4} S/m, one or two orders magnitude higher than that of pentacene. Syntheses of heptacene,[102] octacene, and nonacene[103] have also been reported in the literature. Unfortunately, these unsubstituted higher acenes are not stable in ambient environments and their charge transport properties could not be obtained. Interestingly, a dihydrotetraazaheptacene derivative with ambient stability for 3 years has recently been published.[104] Unfortunately, the solubilizing groups utilized interfered with the $\pi-\pi$ overlap of adjacent molecules, a testament to the complicated nature of achieving ambient stability and performance.

The electronic properties of acenes strongly rely on their molecular packing structures. On the basis of their crystal structure data, Table 1 summarizes reorganization energies, transfer integrals (electronic coupling t^+) and calculated mobilities of these acenes.[101] It can be seen that the theoretical field-effect mobilities of acenes increase with the number of benzene rings, which is the result of smaller reorganization energies and larger transfer integrals. Therefore, the corresponding experimental results are in good agreement with theoretical calculations, confirming that conjugation extension in small molecules is a viable approach to improve charge mobility in linear acenes. The trend was also observed for 5-, 6-, and 7-ringed fluorinated heteroacenes.[105]

In practical applications, the choice of the acene core length (Figure 2a) is a combination of theoretical performance limit, chemical stability and ease of processing. The HOMO levels of anthracene, tetracene, pentacene, and hexacene are −5.7, −5.21, −5.14, and −4.96 eV measured by photoemission yield spectroscopy, respectively.[101] This trend indicates higher acenes are more prone to oxidation in air. It was found that there always existed a small amount of 6,13-pentacenequinone (the oxidation product of pentacene) in pentacene, even after repeated sublimation.[32] Hexacene underwent much faster photochemical oxidation in the presence of air than pentacene.[100,101] Moreover, higher acenes require higher temperature for vacuum deposition, which may result in thermal decomposition. The thin film morphology is also strongly dependent on the molecular size: smaller acenes tend to have more three-dimensional growth while the very large acenes tend to give small grains due to lower diffusivity at a given temperature.[106] They are also more difficult to be rendered soluble and require more insulating solublizing groups to dissolve, which may ultimately reduce the mobility of the soluble derivatives. To circumvent these issues, a number of approaches have been reported, including replacement of some benzene rings with other heteroaromatic rings to lower the aromaticity, attaching bulky substituents, and substitution with electron-withdrawing groups. They will be discussed in more detail in later sections.

The benzene rings in acenes can be replaced with thiophene rings to give oligothienoacenes, shown in Figure 2b. Compared to oligoacenes, oligothienoacenes have a lower degree of aromaticity (i.e., the π-electrons are less delocalized). Tetrathienoacene (TTA),[107] pentathienoacene (PTA),[108,109] hexathienoacene (HTA),[109−111] heptathienoacene (HPTA) and octathienoacene (OTA)[111] have been prepared and fully characterized. Electrochemical studies by cyclic voltammetry showed reversible oxidation waves for oligothienoacenes up to eight rings, indicative of the good stability of the produced oxidized species. Even more strikingly, the longer OTA even exhibited the formation of the dication, while TTA and HTA only showed one oxidation process.[111] Because of the diminishing C−H$\cdots\pi$ interactions, the molecular packing expectedly changed from a herringbone for acenes to π-stacked structures for thienoacenes, as suggested by diffraction data.[110] Charge mobility was found to be higher for VD-OFETs of PTA, up to 0.045 cm^2/(V s) versus 0.006 cm^2/(V s) for HTA. The results indicate that extension of π-conjugation is not necessarily a reliable way to improve thin film OFET performance as it is strongly dependent on thin film morphology. In addition to linear acenes and oligothienoacenes, other fused ring systems combining benzene rings and heteroaromatic rings have been designed to maintain the good electrical properties of acenes while improving their stability. For example, anthraceno[2,3-*b*]thiophene (ACT),[113] tetraceno[2,3-*b*]thiophene (TCT),[113] and pentaceno[2,3-*b*]thiophene (PCT)[114] were synthesized, as shown in Figure 2c. TCT showed better stability than pentacene in both electrochemical and optical measurements. The longer PCT, on the other hand, was less stable than pentacene, but was still much more stable than hexacene. VD-OFETs of ACT, TCT and PCT gave charge mobilities of 0.15, 0.47, and 0.57 cm^2/(V s), respectively.

Under similar conditions, sublimation purified pentacene gave a mobility of 0.5 $cm^2/(V\ s)$.[114]

The above strategy can be further extended by replacing two terminal benzene rings to give anthradithiophene (ADT), as shown in Figure 2d. This molecule has a higher barrier for oxidation than TCT because the loss of aromaticity from replacing two benzene rings with two thiophene rings is larger than that for TCT. Indeed, the stability of ADT was greatly enhanced.[115] Unfortunately, the obtained mobilities from VD-OFETs of ADT were around 0.09 $cm^2/(V\ s)$, likely because of the existence of two isomers in the tested ADT compound.

Putting two fused thiophene rings in the middle of the acenes, benzothieno[3,2-*b*]benzothiophene (BTBT), dinaphtho[2,3-*b*:2′,3′-*f*]thieno[3,2-*b*]thiophene (DNTT) and dianthra[2,3-*b*:2′,3′-*f*]thieno[3,2-*b*]thiophene (DATT) was reported,[54,89,112] as shown in Figure 2d. DNTT and DATT are much more stable than pentacene and hexacene, respectively. The HOMO levels of DNTT and DATT thin films measured by photoelectron spectroscopy in air (PESA) were estimated to be −5.4 and −5.1 eV, respectively. VD-OFETs of DNTT and DATT gave charge mobilities of 3.1 and 3.0 $cm^2/(V\ s)$, respectively.[112] Most importantly, the shelf lifetime of the DATT-based OFETs under ambient conditions showed no significant increase in off-current with only slightly reduced mobilities.

The above examples suggest that the combination of conjugation extension and proper lowering of aromaticity is an effective way to achieve high charge mobilities for fused ring systems with good stability. In fact, there are additional examples which have used the above design principles and resulted in stable high performance OSCs, such as *N*-dodecyldinaphthocarbazoles,[116] and benzoannulated fused oligothiophenes and oligoselenophenes (Figure 2e).[117,118]

2.3. Heteroatom Replacement: A Not-so-Straightforward Way To Tune Charge Transport. Heteroatom replacement constitutes an important part of a conjugated core and imposes a big influence on electronic structure and crystal packing of the molecule.[117,118] The successful demonstration of high mobility benzothienoacenes is a good example. Figure 3 exhibits a few examples of heteroatom replacement ranging from chalcogen atoms, to nitrogen and carbon atoms. The effect of switching from sulfur to selenium was marginal in the case of quaterthiophene[46] and quaterselenophene,[119] as shown in Figure 3a. In 2,6-diphenylbenzodichalcogenophenes (DNTT/DNSS), however, the replacement of sulfur with selenium had a big impact on the charge mobility rising from 0.081 to 0.17 $cm^2/(V\ s)$.[120] Unexpectedly, the trend did not continue when changing from selenium to tellurium, and the mobility dropped about 2 orders of magnitude from 0.17 to 0.0073 $cm^2/(V\ s)$. In dinaphthochalcogeno-phenochalcogenophenes, the difference between sulfur and selenium on mobility was minimal.[121] In the series of circulene molecules, however, octathio[8]circulene outperformed tetrathiotetraseleno[8]circulene by nine times in mobility.[122] Other reports also showed a similar outcome.[123] As far as the environmental effect is concerned, however, the higher toxicity of selenium and tellurium actually discourages us to use these compounds in practical applications. Additionally, the chemistry of sulfur is much more versatile than that of selenium and tellurium.

The heteroatom effect between sulfur and nitrogen is rather clear, as seen in Figure 3b. The *anti*-dibenzothienopyrrole (*anti*-DBTP) showed a mobility of 0.012 $cm^2/(V\ s)$ in VD-OFET

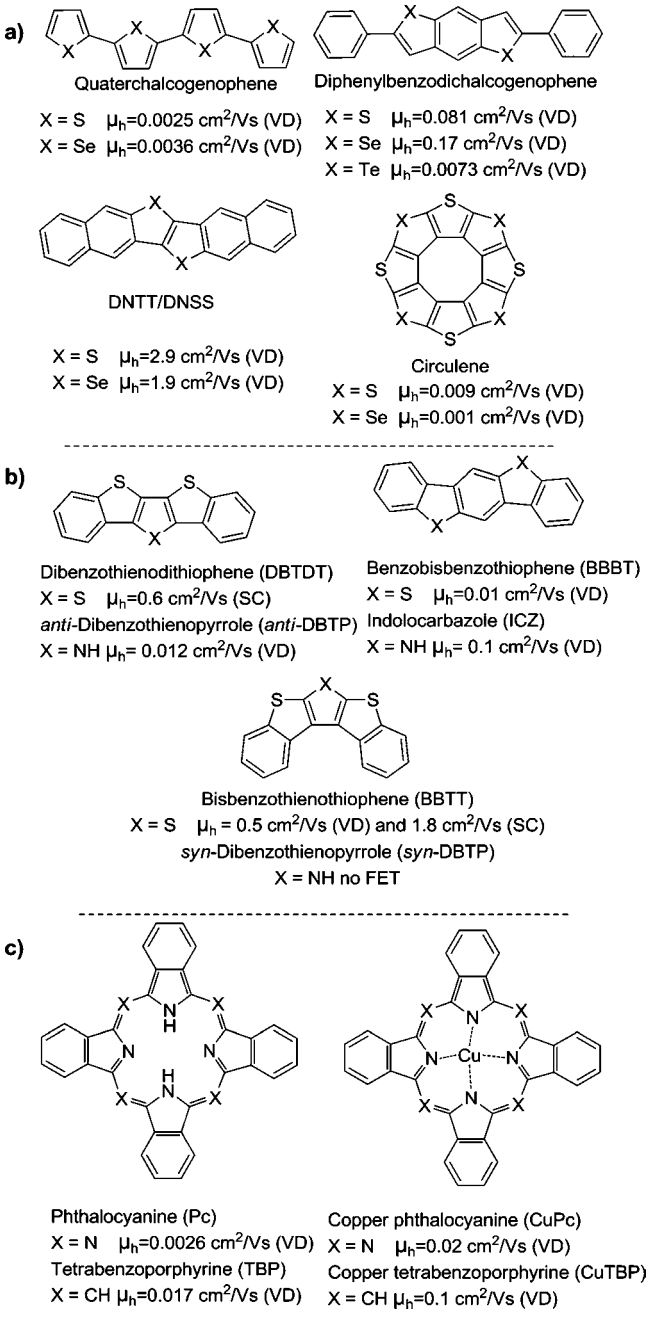

Figure 3. Representative heteroatom replacement in organic semiconductors.

devices,[124] while its sulfur counterpart dibenzo[*d*,*d*′]thieno[3,2-*b*;45-*b*′]dithiophene (DBTDT) gave a mobility of 0.6 $cm^2/(V\ s)$ in SC-OFET devices.[125] The *syn*-dibenzothieno[*b*,*d*]pyrrole (*syn*-DBTP) did not even exhibit any field effect behaviors,[124] while the sulfur version (BBTT) exhibited a mobility of 0.5 $cm^2/(V\ s)$ in VD-OFET devices and 1.8 $cm^2/(V\ s)$ in SC-OFET devices.[126] However, the introduction of N−H···π interactions in a favored manner can result in an increase in mobility. Such N−H···π interactions are incorporated in indo[3,2-*b*]carbozole (ICZ),[127] together with C−H···π interactions, in which an ICZ central molecule strongly interacts with four adjacent molecules, which creates an extremely favorable bidirectional electronic coupling in the crystals. VD-OFETs of ICZ gave a satisfying mobility up to 0.1 $cm^2/(V\ s)$. In contrast, its sulfur counterpart, benzo[1,2-*b*:4,5-*b*′]bis[*b*]-

dx.doi.org/10.1021/ja400881n | J. Am. Chem. Soc. 2013, 135, 6724−6746

benzothiophene (BBBT), only exhibited a mobility of 0.01 $cm^2/(V\ s)$.[45]

Phthalocyanines (*Pc*) are the counter version of porphyrins when bridged nitrogen atoms are replaced with sp^2 carbons. An increase in charge mobility in OFET devices was often reported, as shown in Figure 3c.[25,128−130] This phenomenon also holds true in linear acenes when some of the carbons are replaced with nitrogen atoms.[131,132] To further extend this observation to other systems, however, more examples are needed. Additionally, replacement of an sp^2 carbon with nitrogen can lead to n-type charge transport properties.[133,134]

2.4. Core Substitution with Electron Withdrawing Groups: A Venue to Air Stable n-Type Charge Transport. An electron withdrawing group, such as F, Cl, Br, and CN, can pull electron density away from a π-conjugated system either through a resonance or inductive effect. Substitution on a conjugated core with electron withdrawing groups generally leads to enhanced stability toward oxidation, a potential transition from p-type materials to ambipolar or n-type materials, and a change in molecular packing. One of the hurdles that the organic electronic community has to overcome has been the development of n-type OSCs with operational stability under ambient conditions to complement high performance p-type materials for making organic integrated circuits. To that end, designing OSCs with low lying LUMO levels (below −3.8 eV) is needed to achieve operational stability in air.[92,135,136] On the contrary, electron donating groups, such as alkoxy or alkyl thioether, typically increase oxidation potential and reduce stability. In this section, we highlight the effects of core-substitution with electron withdrawing groups.

Fluorination is one of the most popular approaches to achieve air-stable n-channel OSCs. Hexadecafluorocopper phthalocyanine ($F_{16}CuPc$) is one of the first high performance air-stable n-channel OSCs that showed measured VD-OFET mobility greater than 0.01 $cm^2/(V\ s)$.[137] A similar strategy was applied to pentacene. Perfluoropentacene has an increase of about 0.6 eV in ionization energy and about 0.7 eV in electron affinity, indicating a better air stability and ease of electron injection.[138] While the packing motif did not change from copper phthalocyanine to $F_{16}CuPc$, perfluoropentacene has significantly different crystal packing from pentacene as shown in Figure 4. From a theoretical perspective, DFT computational studies indicated that the intramolecular reorganization energies were doubled and the average transfer integral was found to be nearly equal from pentacene to perfluoropentacene, suggesting the intrinsic hole and electron mobilities might be lower in perfluoropentacene.[139] Theoretical calculations also suggested that larger electronic couplings existed for holes than for electrons, but similar electron−phonon couplings exist for perfluorinated crystals, implying the possibility for these materials to act as ambipolar transporters. Experimentally, VD-OFETs of perfluoropentacene gave an electron mobility of 0.11 $cm^2/(V\ s)$.[138] No p-type charge transport was reported in this study for perfluoropentacene.

Instead of perfluorination, partial fluorination can result in ambipolar charge transport. For example, 5,12-bis(triisopropylsilylethynyl)tetraceno[2,3-*b*]thiophene (TIPS-TCT) and 7,8,9,10-tetrafluoro-5,12- bis(triisopropyl-silylethynyl)-tetraceno[2,3-*b*]thiophene (TIPS-FTCT) (as shown in Figure 5a) were prepared and tested in OFET devices. TIPS-TCT showed typical p-type charge transport, and an average mobility of 0.80 $cm^2/(V\ s)$ with a maximum mobility of 1.25 $cm^2/(V\ s)$.[140] Upon fluorination, TIPS-FTCT exhibited ambipolar charge transport properties, with an electron mobility of 0.37 $cm^2/(V\ s)$ and a hole mobility of 0.12 $cm^2/(V\ s)$.[141] Ambipolar charge transport behavior exhibited by TIPS-FTCT is in good

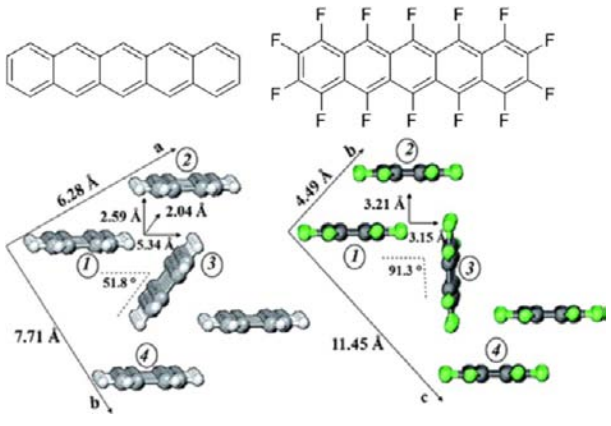

Figure 4. Illustration of the lattice parameters with the ab layer of single crystal of pentacene and the bc layer of perfluoropentacene. Reproduced with permission from ref 139. Copyright 2009 American Chemical Society.

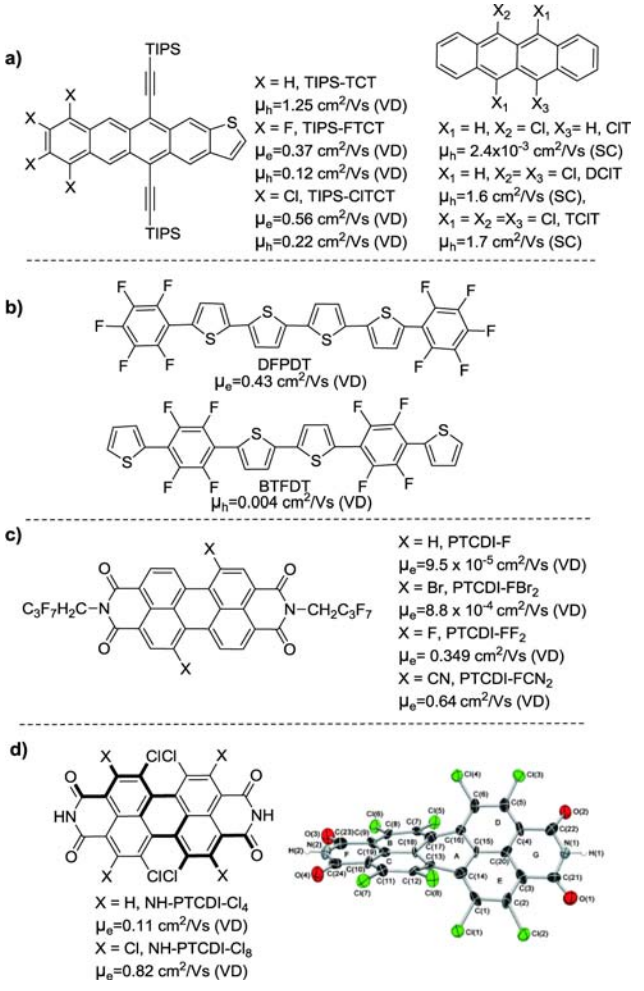

Figure 5. Representative halogenated organic semiconductors and the crystal structure of NH-PTCDT-Cl_8. Reproduced with permission from ref 147. Copyright 2010 WILEY-VCH Verlag GmbH & Co.

dx.doi.org/10.1021/ja400881n | *J. Am. Chem. Soc.* 2013, 135, 6724−6746

agreement with the theoretical calculations.[139] The HOMO level of TIPS-FTCT is about 0.2 eV deeper than that of TIPS-TCT, making it an air-stable high performance ambipolar molecule. In addition to fluorination, chlorination was found to be even more effective in lowering the LUMO level of the resulting molecules, most likely due to the fact that a chlorine atom contains empty 3d orbitals that can accept π-electrons from the conjugated core, while F does not have energetically accessible empty orbitals for such delocalization.[142] For example, replacing fluorine atoms with chlorine atoms was found to reduce the LUMO of TIPS-ClTCT by 0.1 eV.[142] A detailed review on effects of halogenation on the properties of OSCs can be found elsewhere.[143]

In the previous examples, halogenation was on the terminal rings. One important question is whether the positions of substitution would affect the nature of charge transport. The next two examples will shed some light on this question. 5-chlorotetracene (ClT), 5,11-dichlorotetracene (DClT) and 5,6,11,12-tetrachlorotetracene (TClT) were obtained and tested in OFETs,[144,145] as shown in Figure 5a. It is reasonable to expect that TClT at least would exhibit ambipolar or n-type charge transport properties, judging from the previous examples. However, none of these molecules showed n-type charge transport properties. Instead, DClT and TClT displayed rather good hole single crystal mobilities of 1.6 and 1.7 $cm^2/(V\ s)$, respectively. As the authors proposed, on the other hand, halogenation indeed changed the crystal packings from a herringbone-type structure for ClT to a face-to-face slipped π-stacking motif for DClT and TClT, which might contribute to the difference in their charge transport.

In another example, two oligothiophenes of 5,5″-diperfluorophenyl-2,2′:5′,2″:5″,2‴-quaterthiophene (DFPDT) and 5,5′-bis[1-[4-(thien-2-yl)perfluorophenyl]]-2,2′-dithiophene (BTFDT) were prepared,[146] as shown in Figure 5b. These two oligomers have similar LUMO levels. Interestingly, DFPDT exhibited n-type charge transport behavior, with mobility as high as 0.43 $cm^2/(V\ s)$, while BTFDT displayed p-type transport behavior, with a relatively low mobility of 0.004 $cm^2/(V\ s)$. It is obvious that the position of substitution does play an important role on charge transport and crystal packing.

The most studied air-stable n-channel OSCs are perhaps perylene diimide and naphthalene diimide derivatives. With additional electron withdrawing substitution on these already electron-deficient molecules, many high mobility air-stable n-channel OSCs have been reported.[92] Some of the perylene diimides are listed in Figure 5c. The addition of highly electron-withdrawing groups, such as −CN and −F, on the PTCDI core lowers the LUMO levels below that of most atmospheric trapping species, which, together with a close-packed solid state resulting from fluorinated substituents at the N,N′-positions, rendered ambient stability to PTCDI-F2 and PTCDI-CN2.[148] In contrast, the parent and bromo-substituted PTCDI OFETs did not exhibit good n-type charge transport mobility and operational air-stability.[135] After a comprehensive investigation, it was concluded that minimizing geometric distortions of the arylene skeleton caused by electron-withdrawing substituents is essential in order to retain close molecular packing and high air stability. Additionally, the morphological effect is also important to consider as air stability is the outcome of both thermodynamic (molecular energy levels) and kinetic (diffusion of oxygen and water into the films) influences.[92,135] Interestingly, severe conjugated core distortion by high chlorination of the perylene diimide core was designed to result in a two-dimensional $\pi-\pi$ stacked percolation path for electron transport. The resulting compound, NH-PTCDI-Cl_8 showed air-stable n-channel thin film VD-OFET mobilities as high as 0.82 $cm^2/(V\ s)$.[147] The dark line indicates the twisting core and its crystal structure is shown in Figure 5d.

2.5. Side Chain Engineering: A Roundabout Strategy To Influence Charge Transport. Side chains on conjugated cores primarily function as solubilizing groups to impart the solution-processability to OSCs. They are considered as insulating materials, and do not contribute to charge transport directly. It has been increasingly more recognized, however, that side chains have a substantial impact on charge transport through affecting molecular packing and thin film morphology in solid states.[149−153] In this section, we highlight some intriguing discoveries on side chain engineering and their influence on charge transport.

In acenes, alkylation or arylation of peri-positions has been introduced to improve stability against oxidation and prevent dimerization of the molecules. These substitutions also changed packing motifs from herringbone to face-to-face π-stacking by diminishing C−H···π interactions. Detailed studies on peri-substituents on tetracene and pentacene have been reported.[86,154,155] It was proposed that the length and bulkiness of the substituents govern the molecular arrangements of the materials and argued that a 2D face-to-face structure would be rendered if the substituent length is approximately half of the acene core.[86,154] Figure 6a displays examples of such structures

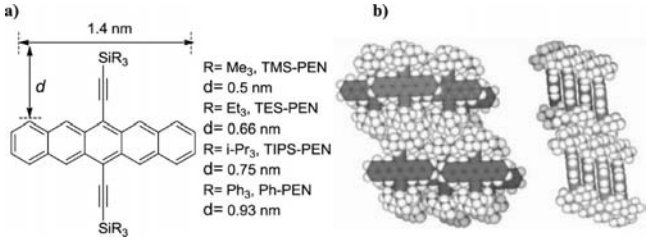

Figure 6. (a) Chemical structures of 6,13-subsititued pentacene and (b) packing motif of TIPS-PEN. Reproduced with permission from ref 154. Copyright 2001 American Chemical Society.

based on the pentacene core. Other than Ph-PEN, all the derivatives adopted 2D face-to-face arrangements in single crystals as shown in Figure 6b, while their parent core pentacene is known to have a herringbone structure. SC-OFETs of TIPS-PEN, with a 2-D bricklayer structure, gave mobilities as high as 3.8 $cm^2/(V\ s)$.[88] A similar strategy has been applied to other acene derivatives for both p- and n-type thin film transistors.[133,134,140,156−158]

Similar with the cases of halogen substitution, crystal packing is also sensitive to the position of alkylation. For example, DNTT (Figure 7) adopts a typical herringbone arrangement and has a mobility up to 2.9 $cm^2/(V\ s)$ in VD-OFETs.[159] In contrast, 2,9-DMDNTT shows a so-called "3D-herringbone packing mode",[159] while 3,10-DMDNTT exhibits another molecular arrangement. However, the change of packing did not reflect much in charge transport. VD-OFETs of 2,9-DMDNTT and 3,10-DMDNTT displayed good mobilities of 0.8 and 0.4 $cm^2/(V\ s)$, respectively.

The effects of asymmetric alkylation on molecular packing and thin film morphology have also been investigated, complementary to the aforementioned symmetrical substitution.[3,160,161] Fluorene-bithiophene-fluorene (FTTF), together

dx.doi.org/10.1021/ja400881n | J. Am. Chem. Soc. 2013, 135, 6724−6746

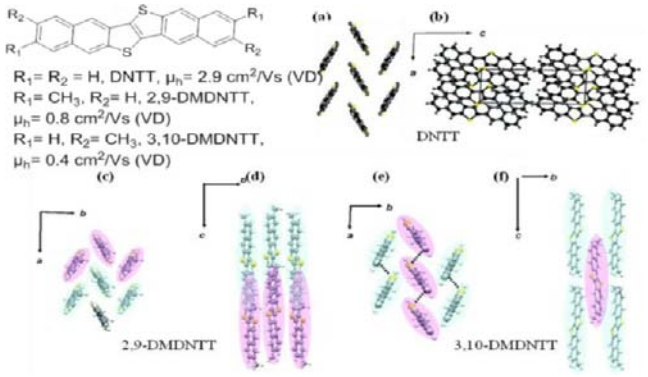

Figure 7. Packing motifs of dinaphtho[2,3-*b*:2′,3′-*f*]thieno[3,2-*b*]-thiophene (DNTT) derivatives (crystal structures a–f are reproduced with permission from ref 159. Copyright 2010 Royal Society of Chemistry).

with its symmetrically and asymmetrically alkylated derivatives has been examined (Figure 8a).[23,161,162] It was found that the addition of the alkyl chains did not change the molecular packing motif. Interestingly, the conjugated core of FTTF in the asymmetric derivatives is in direct contact with the substrate surface, and its single alkyl chain is aligned away from that interface, making the FTTF core distribution near the dielectric interface different from its symmetric counterparts.

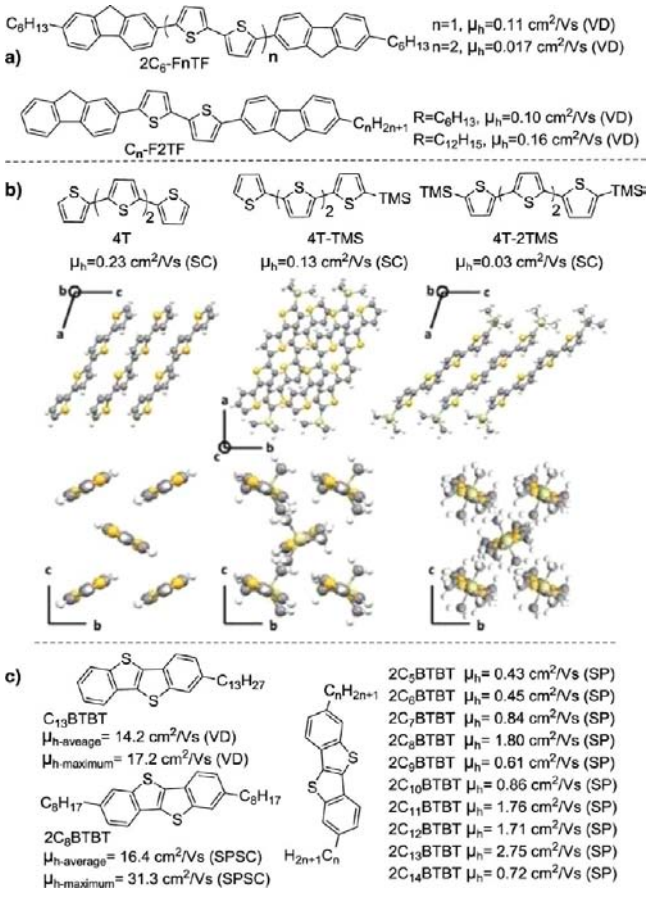

Figure 8. The effect of alkyl chain symmetry and length on molecular packing and charge transport (crystal structures in inset (b) are reproduced with permission from ref 160. Copyright 2009 WILEY-VCH Verlag GmbH & Co).

Additionally, it was found that the alkyl chain size (e.g., molecular aspect ratio) plays a significant role in 2D and 3D polycrystallite formation, which directly affects the charge mobility.[161]

In the investigation of asymmetric and symmetric oligothiophenes bearing bulkier terminal trimethylsilane (TMS) groups, it was found that the herringbone crystal packing motif remained the same while the lattice constants changed significantly, as shown in Figure 8b.[160] For the 4T-TMS, the alternating TMS groups between layers allow the oligothiophene cores to arrange nearly vertically, so as to arrange the bulky groups in nearly equidistant, space-filling fashion. In contrast, the 4T-2TMS is unable to accommodate twice the density of TMS groups between layers in an upright position, and the molecule must tilt severely to stagger the units. Thus, the asymmetric derivative outperformed the symmetric one in terms of SC-OFET mobility.[160] The asymmetric side chain strategy has also been adopted on benzothieno[3,2-*b*][1]-benzothiophene (BTBT), as shown in Figure 8c. The resulting C_{13}-BTBT demonstrated a high thin film mobility of 17.2 $cm^2/(V\ s)$ with an average mobility of 14.2 $cm^2/(V\ s)$ in VD-OFETs, significantly higher than 2.75 $cm^2/(V\ s)$ of its solution-processed symmetric alkylated BTBT derivative ($2C_{13}$–BTBT).[3,54]

The length of the alkyl chain exerts its influence on charge transport in the form of the "molecular aspect ratio" and the "odd-even" effect. We briefly discussed the impact of molecular aspect ratio in the FTTF molecules.[23] The odd–even effect has also been studied in OSCs. A set of 10 BTBT molecules from $2C_5$-BTBT to $2C_{14}$-BTBT have been synthesized and tested in SP-OFETs, as shown in Figure 8c.[54] From C_5 to C_{10}, the even-numbered derivatives outperform the odd-numbered derivatives, while the trend is reversed from C_{10} to C_{14}. Clearly, the odd–even effect does not solely dominate the charge transport. The outcome is a result of the combined force between the molecular aspect ratio and the odd–even effect. In addition, the outcome of the odd–even effect is also dependent on the underlying substrate.[163]

Other than the attachment of alkyl chains onto carbon atoms, N-alkylation is often used to introduce solubilizing groups when the conjugated core contains nitrogen atoms. However, this attachment could potentially block N–H$\cdots\pi$ interactions and change molecular packing. Such examples are displayed in Figure 9. As pointed out earlier, the synergy of N–H$\cdots\pi$ and C–H$\cdots\pi$ interactions in ICZ crystals resulted in strong bidirectional electronic coupling, facilitating charge transport.[127] When the nitrogen atom was capped by a phenyl group, the resulting *N*,*N*′-bis(*p*-octylphenyl)indolo[3,2-*b*]-carbazole (OPICZ) adopts a co-facial π-stacking pattern as a result of the loss of N–H$\cdots\pi$ interactions, as seen in Figure 9a,b. In thin films, ICZ adopts a head-on orientation relative to the substrate while OPICZ molecules are parallel to the substrate. The influence of N–H$\cdots\pi$ interactions on molecular packing and film structure was seen as the observed differences in device performance. VD-OFETs of ICZ and OPICZ exhibited charge mobilities of 0.1 and 0.01 $cm^2/(V\ s)$, respectively. This similar influence might also be present in pyrrolobis-benzothiazine (PBBT, Figure 9), even though the authors did not explicitly describe it.[164] The parent PBBT displayed mobilities as high as 3.6 $cm^2/(V\ s)$ in SC-OFETs, likely due to the existence of 2D charge transport channels. The N-alkylated derivatives exhibited much smaller mobilities because of 1D transport properties. Utilization of intra-

dx.doi.org/10.1021/ja400881n | J. Am. Chem. Soc. 2013, 135, 6724–6746

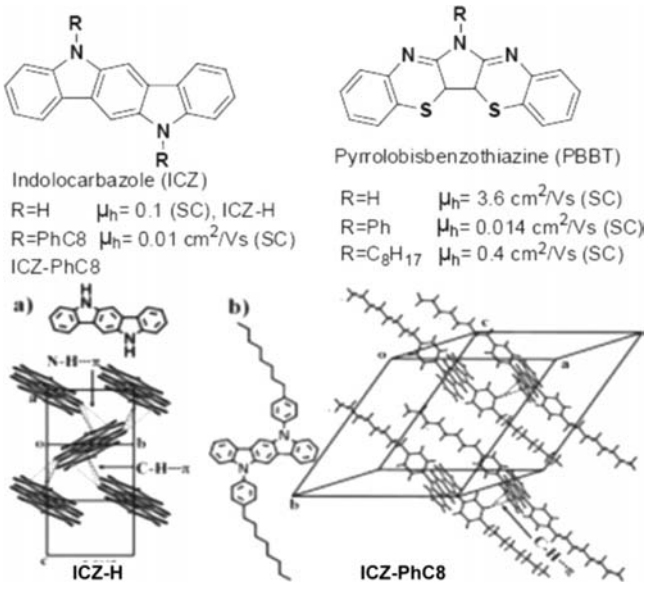

Figure 9. Chemical structures of representative molecules with hydrogen-bonding and their molecular packing (crystal structures are reproduced with permission from ref 127. Copyright 2009 WILEY-VCH Verlag GmbH & Co).

molecular or intermolecular hydrogen-bonding to promote desirable crystal packing has been observed in other conjugated systems.[165−167]

In addition to alkyl chains, hydrophilic triglyme chains and other oligo ethers have also been used as side chains in conjugated molecules.[149,168] When both hydrophilic triglyme and hydrophobic alkyl chains are substituted on the same conjugated core, termed as the amphiphilic molecular design,[149,169] some unique features (e.g., plastic crystal phase) were found and may sometimes have a beneficial impact on charge transport.[168] Aryl groups, in some cases, were also used as side chains to tune molecular packing. For example, phenyl and perfluorophenyl groups were placed onto tetracene at the 5- and 11-positions to induce a close face-to-face stacking of the tetracene cores.[170] Fluoroalkyl chains were often selected for their electron-withdrawing effect and their dense packing, leading to air stable n-channel transport.[135,171]

The linear side chains we discussed above usually do not impart good enough solubility for various printing techniques. In this regard, branched side chains are attractive. Unfortunately, branched chains tend to disrupt crystal packing and give poor mobilities. To solve these issues, thermally cleavable side chains were introduced, such as an aliphatic carbonyloxy substituent onto sexithiophene. Upon thermal treatment, the carbonyloxy group was volatilized and two short hydrocarbon chains were left at the end thiophene rings.[51] Mobilities around 0.1 $cm^2/(V\ s)$ were obtained for these thermocleavable oligothiophenes.[51,172−175] Recently, the cleavable side chain concept was applied to otherwise highly insoluble quaterrylene diimides by attaching cleavable swallow-tailed side chains. They turned a sparingly soluble quaterrylene diimide into a highly soluble molecule for solution shearing. Electron mobility up to 0.088 $cm^2/(V\ s)$ was obtained for this molecule upon cleavage.[176] Another unique side chain is the cyclohexyl group, which has been frequently used in PTCDI and other molecules.[177] The cyclohexyl group adds steric bulkiness at the periphery of the molecule, which provides for improved solubility without having a detrimental effect on the molecular packing in the thin film phase. Additionally, bulky substituents in cyclohexane tend to adopt equatorial positions,which should further increase the conformational rigidity of the overall molecule.[178] A record high n-type mobility of 6 $cm^2/(V\ s)$ was achieved on naphthalene diimides bearing two cyclohexyl groups.[178]

2.6. Conjugated Polymers: More than Just Linking Small Molecules Together. In the previous sections, we have introduced some general design strategies applied to small molecule OSCs. Conjugated polymers consist of chains of small molecules (monomers). It is not surprising that some of the above molecular design principles have also been collectively applied to conjugated polymers. We already discussed briefly the evolution of polymer semiconductor development in section 1.1.

Here, we discuss additional polymer design considerations using isoindigo-based polymers as examples shown in Figure 10. Even though isoindigo has been a well-known molecule for

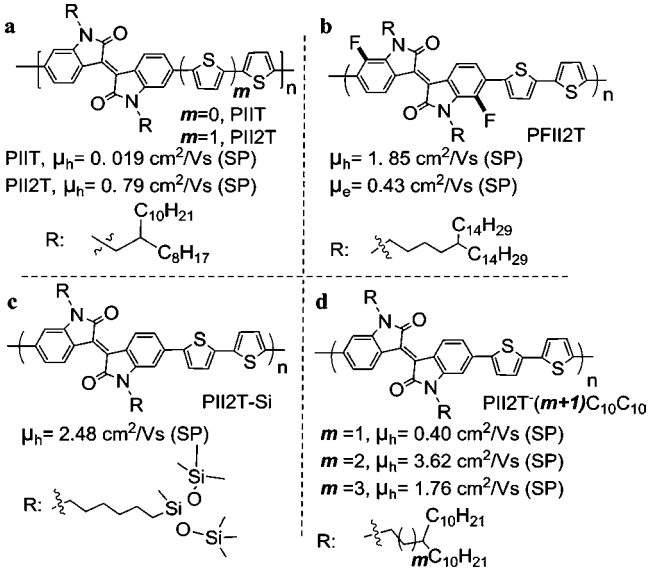

Figure 10. Molecular engineering in isoindigo-based conjugated polymers.

dyes and pigments, its use as an electron deficient unit for donor−acceptor polymers became popular recently.[179] Similar strategies as those we discussed concerning small molecules have also been applied to obtain high performance OFET isoindigo-based polymers (PII). For example, PIIT and PII2T (Figure 10a) showed very different charge transport properties with mobilities of 0.019 and 0.79 $cm^2/(V\ s)$, respectively.[67] The authors attributed the difference to better molecular packing, C2 symmetry, and high molecular weight of PII2T. Core substitution with electron-withdrawing groups, such as fluorinated isoindigo, PFII2T (Figure 10b), was also proven to be effective in conjugated polymers in lowering their LUMO levels.[180−184] Not surprisingly, the substitution not only led to excellent electron mobilities as high as 0.43 $cm^2/(V\ s)$, but also enhanced the hole charge transport properties as well with mobilities up to 1.85 $cm^2/(V\ s)$, due to stronger interchain interactions. Additionally, the introduction of fluorine atoms improved device storage and operational stability under ambient conditions.

Side chain engineering (e.g., position, length, shape and type) has been extensively practiced in conjugated polymers for

dx.doi.org/10.1021/ja400881n | J. Am. Chem. Soc. 2013, 135, 6724−6746

OFETs,[64,185−189] including isoindigo-containing polymers. In the original PII2T, the polymer was rendered soluble by introducing bulky branched side chains. However, the bulkiness of the side chains resulted in a larger $\pi-\pi$ stacking distance between the conjugated backbones, which has a dramatic impact on electronic coupling, and thus charge carrier mobility.[96] To address the issue,[69,190] a siloxane-terminated hexyl chain was designed to replace the 2-octyldodecyl side chain in order to move the bulky branching point away from the conjugated backbone, as seen in Figure 10c. This strategy worked very well in reducing the $\pi-\pi$ stacking distance from 3.75 Å with 2-octyldodecyl side chains to 3.58 Å with the siloxane chains, measured by grazing incidence X-ray diffraction (GIXD). A mobility as high as 2.48 $cm^2/(V\ s)$ was observed for PII2T-Si.[69] Dithienyl-diketopyrrolopyrrole and selenophene containing polymers were subsequently reported with such hybrid siloxane-solubilizing groups (not shown here).[191] Both high hole and electron mobilities of 3.97 and 2.20 $cm^2/(V\ s)$, respectively, were found for these polymers. A systematic study was recently reported in which a series of PII2T-$(m + 1)C_{10}C_{10}$ (Figure 10d) were synthesized to investigate the effects of moving the branching point away from the conjugated backbone. The $\pi-\pi$ distances were found to be 3.75, 3.61, 3.57, and 3.57 Å for PIIT, PII2T-$2C_{10}C_{10}$, PII2T-$3C_{10}C_{10}$, and PII2T-$4C_{10}C_{10}$, respectively. A mobility as high as 3.62 $cm^2/(V\ s)$ was reported for the PII2T-$2C_{10}C_{10}$ SP-OFETs.

Conjugated polymers are more than just linking small molecules together. In particular, even though sharing the same repeating units, the molecular weight of the polymer can have a dramatic impact on the charge transport properties of the resulting polymer due to the changes in dominating the charge transport mechanism of intra- versus intermolecular charge transport, as well as changes in thin film morphology.[192] In addition, their packing behaviors could be drastically different from their corresponding small molecules, considering the conformational complexity of the polymer chains. It is therefore very important to select appropriate repeat units, in particular in donor−acceptor (D-A) type conjugated polymers. Here, we use a few selected examples to illustrate the significance of repeating unit construction and its influence on molecular packing in conjugated polymers.

A set of 10 isoindigo-based polymers were classified into two categories based on their backbone symmetry and curvature by Pei and co-workers, namely centrosymmetric and asymmetric polymers,[68] as shown in Figure 11. Different lamellar packing and crystallinity were found for these polymers based on their backbone symmetry as revealed by AFM and GIXD measurements. A high degree of ordering was typically observed when the polymers are centrosymmetric and it further improves upon annealing. In sharp contrast, all polymers containing asymmetric donor blocks showed little or no out-of-plane diffractions, suggesting the absence of lamellar packing in these polymer thin films. On the basis of this information, the authors proposed a "molecular docking" concept. The OFET performance was found to correlate well with the proposed "molecular docking" strategy. The performance of centrosymmetric polymers in general are orders of magnitude higher than those of axisymmetric polymers. A similar observation was found for six polymers consisting of the structural isomers dithieno[2,3-*b*;7,6-*b*]carbazole or dithieno[3,2-*b*;6,7-*b*]-carbazole with three different acceptors.[193] They suggested that pseudo-linearly shaped backbones usually lead to enhanced OFET mobilities. Very recently, a DPP-based donor−acceptor

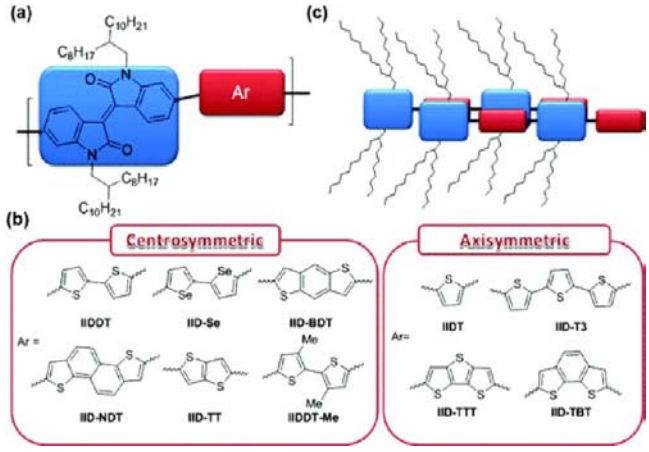

Figure 11. (a) Structures of isoindigo-based copolymers; (b) centrosymmetric and axisymmetric donor of the copolymers; (c) proposed interpolymer docking model, reproduced with permission from ref 68. Copyright 2012 Chemical Society.

conjugated polymer gave a record high mobility over 10 $cm^2/(V\ s)$ from SP-OFETs.[5] Coincidentally, this polymer also has a centrosymmetric co-monomer.

The design principles learned from small molecules have been extensively applied to conjugated polymers, such as core extension,[61,194−196] electron-withdrawing group substitution,[180−184] side chain engineering[150,185−188] and heteroatom replacement.[197,198] On the other hand, it has to be pointed out that polymers are different from their individual monomers in physical properties. The physical properties of polymers (e.g., symmetry,[68] molecular weight,[5,199] and donor−acceptor interaction[64]) play an important role in polymer OFETs.

2.7. Thinking Outside the Box: Unconventional Organic Semiconductors. So far, we have mainly discussed one-dimensional (1D), (pseudo)linear OSC cores. There are also considerable research efforts toward 2D-shaped molecules (e.g., coronenes,[168,200−204] triphenylenes,[205−207] phthalocyanines,[11,208−210] extended rylenes,[211,212] and synthetic graphene nanoribbons,[213] displayed in Figure 12) and more complicated structures (e.g., DNA hybrids,[214−216] organic frameworks,[217−219] and grafted polymers[220]) for charge transport.

In general, synthetically tailored 2D OSCs still lag behind 1D OSCs in terms of charge mobility in FETs.[207,210,212,221−223] This is largely due to the difficulty in synthesizing a large amount of such OSCs with high purity, difficulty in processing and controlling morphology and orientation of the molecular stacks.[223] However, some very recent chemical designs show new promise for this class of compounds. For example, an ABAB-symmetric tetraalkyl titanyl phthalocyanine together with side-chain engineering resulted in a 2D slipped $\pi-\pi$ stacking motif in the thin films, and hole mobilities approaching 1 $cm^2/(V\ s)$ in SP-OFETs without thermal annealing were observed.[210]

So far, the charge transport in the OSC systems reviewed above relies primarily on intermolecular charge transport, that is, the charges need to move from one molecule to another to transport through the thin film. However, it has been recognized for a long time that intramolecular charge transport may be significantly faster than intermolecular transport. This was verified both theoretically and experimentally.[192,224,225]

Even though tremendous efforts have been devoted to making single molecule junctions,[226−233] thin film transistor

dx.doi.org/10.1021/ja400881n | J. Am. Chem. Soc. 2013, 135, 6724−6746

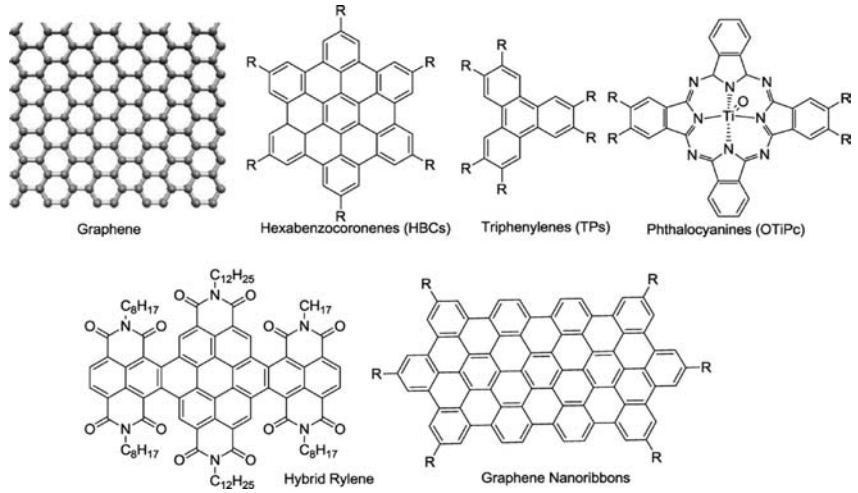

Figure 12. Representative 2D organic semiconductors.

measurements relying on primarily intramolecular charge transfer are still scarce due to the difficulty in device fabrication. However, in some polymer OSC systems, it has been observed that ultrahigh molecular weight resulted in higher charge carrier mobilities.[5,64,234] In addition to the effects of crystallinity, grain connectivity, grain size, and molecular orientation impacted by molecular weight,[5,234−237] an important contribution could be from the increase of the intramolecular charge transport in these systems. In addition, alignment of polymer chains in a liquid crystalline phase is a potentially effective method to enhance the intramolecular charge transport component to increase the bulk material mobility.[238]

To take advantage of the fast intramolecular charge transport, covalent linkage of charge transport units is a potential strategy. A DNA double helix polymer structure represents an example from nature, in which the long-range charge transport along the π-stacked base pairs is assisted by the covalent arrangement on the backbones made of sugars and phosphate groups joined by covalent ester bonds.[214,215] Attempts have also been made to organize conductive or conjugated units as pendant groups from linear polymer backbones, such as polypeptide,[239] double strand poly(norbornene),[240] poly(propargylene),[241] and poly(isocyanide).[242] The electronic transport properties of stacks of perylene-bis(dicarboximide) (PDI) covalently fixed to helical poly(isocyano-peptide)s were studied using thin-film transistors.[220] Although the PDI units were found to organize in a face-to-face stacking manner, the interchain hopping barrier limited the thin film transistor performance as a result of the combined force of less favorable edge-to-edge charge transport between PDI units on different polymer strands and the insulating side chains attached to the polymer backbone.[220]

Recently, a polymer design concept demonstrated a potential approach to take advantage of intramolecular charge transport through covalent attachment of conducting units, as seen in Figure 13. Fullerene (C_{60}) units were used due to its large size so that they can be in close contact with each other when the proper polymer backbone and spacer are used.[243] C_{60} side chain polymers with high relative degrees of polymerization up to 1220 and fullerene compositions up to 53% were synthesized by ruthenium catalyzed, ring-opening metathesis polymerization (ROMP), in order to achieve ultrahigh molecular weight[244] of the corresponding norbornene-functionalized monomers. The electron mobility measured for the thin film FET devices from the polymers was more than an order of

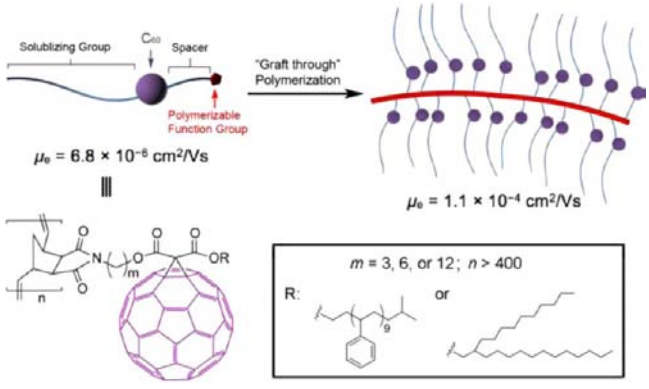

Figure 13. Graphical representation and structural formula of the "graft through" approach to the synthesis of a C_{60} pendant side chain polymer using ring-opening metathesis polymerization. The electron mobility of the resulting polymer is measured to be more than an order of magnitude higher than its monomer.

magnitude higher than that of the monomers even though they were both amorphous. Both the experimental observations and theoretical calculations indicated the strong intramolecular fullerene-fullenrene interactions within the ultra-long polymer chains were responsible for the enhancement.

On the other hand, the organization of conductive units into two-dimensional covalent organic frameworks (COFs) is another approach that may potentially take advantage of intramolecular charge transport.[217,219] COFs are crystalline polymer networks that are covalently joined displaying a long-range order. The synthesis of such an ordered structure relies on the reversible covalent bond formation during the assembly of the network. The charge carrier mobility of porphyrin-based COFs up to 8.1 $cm^2/(V\ s)$ was reported,[219] which was measured on a scale of several nanometers using laser flash photolysis time-resolved microwave conductivity measurements (Figure 14). The fabrication of useful OFET devices using COFs, however, still imposes a challenge because of the difficulty in the processing of these insoluble and nonvolatile materials. Recently, crystalline thin films of COFs have been successfully grown onto graphene substrates from solution through a surface-templated reaction.[245] However, transistor devices have so far not been fabricated using this approach.

dx.doi.org/10.1021/ja400881n | J. Am. Chem. Soc. 2013, 135, 6724−6746

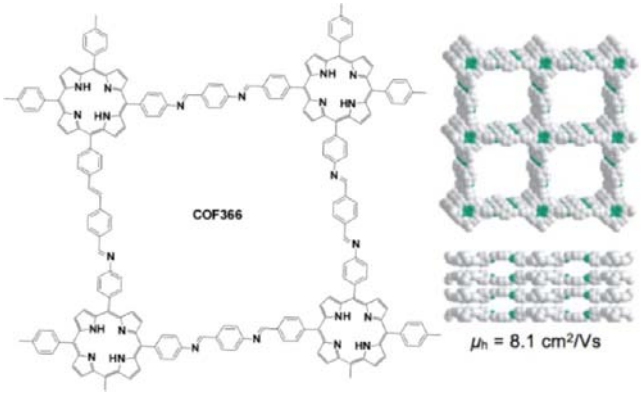

Figure 14. Structural formula and packing mode of COF-366. Reproduced with permission from ref 245. Copyright 2011 American Association for the Advancement of Science.

3. PROCESS ENGINEERING OF ORGANIC SEMICONDUCTORS: A PHYSICAL APPROACH

Molecular design has led to remarkable advances in introducing high-performance and air-stable OSCs.[113,142,246,247] However, the correlation between molecular structure and electronic properties has been complicated by the high sensitivity of charge transport to material processing conditions. Variations of processing parameters, such as substrate chemistry, deposition rate, solvent medium and annealing treatment can lead to field-effect mobility spanning several orders of magnitude in the same material system.[248,249] This phenomenon originates from the complexity of nucleation and crystal growth processes during thin film formation.[151] In typical solution processing methods (spin coating, drop casting, inkjet printing, slot-die coating, etc.),[250,251] crystal formation occurs in a multiphase environment, comprised of solvent vapor, solution layer and substrate. Nucleation and crystal growth are critically influenced by the interactions between solute, solvent and substrate, by the presence of phase boundaries, and by the multiphase mass and heat transport processes. All these parameters jointly determine the morphology and molecular packing of organic semiconductor thin films, which are critical to achieving high electronic performance of a given molecular system.[18,250] On the other hand, such a wide range of processing parameters also presents opportunities for tuning charge transport properties. Below, we survey a few examples.

3.1. Tuning Molecular Packing: Nonsynthetic Approaches. As mentioned earlier, molecular packing strongly influences charge transport in OSC thin films. Previous studies have shown that a slight displacement of or distance between adjacent molecules leads to a significant change in the transfer integral and therefore to the charge carrier mobility.[252]

The molecular engineering approach, whereby the OSC molecular structure is modified to achieve desired molecular packing, has been extensively utilized for attaining desired molecular packing motifs as summarized earlier.[142,147,154,168,253]

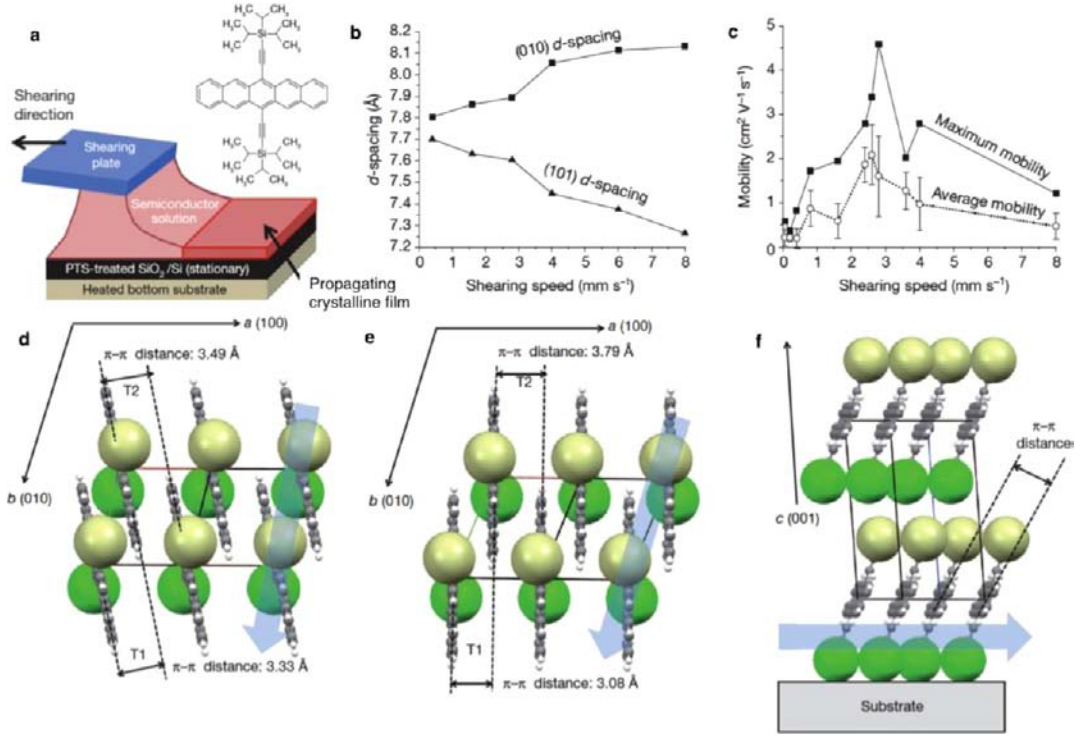

Figure 15. (a) Schematic diagram of the solution-shearing method. (b and c) Lattice strain and charge transport properties as a function of shearing speed. (b) (101) and (010) *d*-spacing of TIPS-pentacene thin films sheared at different speeds. (c) Average and maximum charge carrier mobilities of transistors fabricated from TIPS-pentacene thin films sheared at different speeds. The mobilities were measured along the direction of shearing. The error bars show the standard error of the mean, calculated by dividing the standard deviation of the mobility by the square root of the total number of samples measured. (d–f) Molecular packing structure of TIPS-pentacene thin films prepared under different conditions. (d), Evaporated thin film. (e) A thin film fabricated from solution shearing at a speed of 8 mms^{-1}. T1 and T2 denote the unique molecular pairs. (f), Solution-sheared thin film at 8 mms^{-1}, viewed along the cofacial axis. Spheres represent the TIPS groups: yellow and green correspond to the front and back of the pentacene moiety, respectively. The blue arrow represents the high charge transport direction, as well as the direction of shearing. Reproduced with permission from ref 273. Copyright 2011 Nature Publishing Group.

dx.doi.org/10.1021/ja400881n | J. Am. Chem. Soc. 2013, 135, 6724–6746

However, intense synthetic efforts are required together with the testing of a large amount of candidates in near limitless parameter space. Other less explored methods include the cocrystal approach[254−258] and the interfacial engineering approach,[259−263] which have been recently surveyed by Li et al.[264] and Lee et al.[265]

Molecular packing can also be altered by varying processing conditions, which is made possible by the presence of multiple crystal structures of the same OSC compound, a.k.a. polymorphs. Compared with inorganic semiconductors, OSC crystals are characterized by weak intermolecular interactions, e.g., $\pi-\pi$ stacking, quadrupole interactions,[266] etc. Such weak intermolecular interactions allow one material to assume more than one polymorphic form, which are accessible under typical processing conditions. Examples of OSCs exhibiting polymorphism include pentacene,[267,268] rubrene,[269] fluorinated 5,11-bis(triethylsilylethynyl) anthradithiophene (diF-TES-ADT),[270] and TIPS-PEN,[56,271] just to name a few. Some polymorphs arise from intrinsic material properties (e.g., diF-TES-ADT); some forms are surface-induced thin film phases, which differ from the molecular packing of the bulk crystal (e.g., thiotetracene[272]). Polymorphism can also be categorized in terms of thermodynamic properties. Enantiotropic systems exhibit crystal forms whose stability switch reversibly across a transition temperature below the melting point (e.g., TIPS-PEN[271]). However, a monotropic system possesses only one stable crystal form and the transition between polymorphs is irreversible. Importantly, thermodynamic and structural information on crystalline phases of an OSC system are often missing due to the challenge in characterizing nanoscopic thin films. It is highly likely that many OSCs reported possess polymorphic forms yet to be discovered. It is believed that "the number of forms known for each compound is proportional to the time and money spent in research on that compound."[274]

Despite the importance of molecular packing on charge transport properties, rational approaches for controlling polymorphism are few, and most reported systematic studies concentrated on pentacene polymorphs deposited from the vapor phase. Approaches employed for controlling the pentacene polymorphs include the tuning of film thickness,[275,276] substrate chemistry and temperature,[29,261,277] the ordering states of the SAM interlayer on which pentacene is deposited,[262] and the solvent used for postdeposition annealing,[278] etc. Compared with vapor phase deposition, molecular packing control during solution processing poses additional challenges. The OSC molecular self-assembly processes are complicated by the presence of solvent molecules and the dynamics of fluid flow. How these factors impact molecular packing in OSC thin films are yet to be elucidated. However, solution processing offers unique opportunities for controlling molecular packing. A recent study reported tuning the $\pi-\pi$ stacking distance of OSCs systematically by simply varying the solution processing conditions via solution shearing (SS) (see Figure 15).[56,279] The OSC used for demonstrating this concept was TIPS-PEN, which has been extensively studied as an air-stable, solution processable, and high mobility compound (Figure 14a).[280,281] With this method, the authors were able to reduce the $\pi-\pi$ stacking distance of TIPS-PEN to an unprecedented 3.08 Å (Figure 15d−f). Correspondingly, the charge carrier mobility measured by a field-effect transistor (FET) structure was increased from 0.8 $cm^2/(V\ s)$ for unstrained films (equilibrium polymorph) to as high as 4.6 $cm^2/(V\ s)$ in strained films (a metastable polymorph) (Figure 15c). The high mobility obtained was attributed to the improved electronic coupling between molecules in the strained films supported by density functional theory calculations. As a reference, the previously reported maximum mobility for a TIPS-PEN TFT was 1.8 $cm^2/(V\ s)$.[87] This study points the way to a powerful yet simple nonsynthetic approach for tuning molecular packing of solution processable OSCs. As for the mechanism of strained lattice formation during SS, the authors hypothesized that the fast crystallization and solvent evaporation result in kinetically trapped metastable states favorable for charge transport. A kinetic perspective for controlling molecular packing was also presented in a recent study.[282] The authors prepared thin films of dihexyl-terthiophene using various solution processing methods as well as vapor deposition. They found that slow crystallization speed induces preferential growth of the stable bulk structure, while fast crystallization leads to the occurrence of a metastable thin-film phase, regardless of the processing method used.

The aforementioned studies made significant headway toward rational design approaches for controlling OSC polymorphism using processing techniques. Nonetheless, several key questions remain to be addressed. (1) How to simultaneously achieve desired molecular packing and film morphology in a single step? Figure 15c illustrates the trade-offs between controlling molecular packing and thin film morphology. In this example, lattice strained TIPS-PEN was obtained at high solution shearing speed; however, high shearing speed also led to the formation of smaller and less oriented crystallites. (2) How do different polymorphs emerge and evolve during OSC thin film formation affected by various processing parameters? Key insight into the physical origin of OSC polymorphism can be expected from *in situ* grazing incidence X-ray diffraction studies. Such powerful *in situ* X-ray techniques have been applied to understanding the solvent vapor annealing effect on pentacene films[283,284] and polymer-fullerene blends.[285,286] (3) Can one predict the polymorphic forms of a given OSC and their electronic properties? *A priori* determination of molecular crystal structures has been a long-standing challenge,[287] but will be of tremendous benefit given the time and effort it takes to discover all the polymorphic forms of a given molecular compound. (4) Is high-performing nonequilibrium molecular packing of OSCs sufficiently stable for practical applications? For the TIPS-PEN system it was shown that the nonequilibrium molecular packing is stable for at least a year of storage in the dark under vacuum.[56] New strategies are to be explored to improve the stability of desired crystal polymorphs.

3.2. Single-Crystalline Devices: The Ultimate of Crystal Morphology Control. High performance OTFTs can be fabricated from solution or vapor phase to form polycrystalline thin films, aligned micro crystals or single crystals. Out of various forms of OTFT, patterned single crystals or single-crystalline thin films are favored for several reasons. First, absence of grain boundaries and lack of molecular disorder in single-crystalline domains are essential for achieving high electrical performance. As a result, the best performing OTFTs reported were mostly fabricated as single crystals.[4,74,80] Second, the lack of structural defects and chemical impurities also make single crystals ideal for fundamental studies of intrinsic charge carrier mobility. Third, direct patterning of OTFTs during film formation enables high device density over a large area, and is indispensible for industrial scale production. Direct patterning also ensures a

dx.doi.org/10.1021/ja400881n | J. Am. Chem. Soc. 2013, 135, 6724−6746

high quality dielectric-semiconductor interface, which is critical to excellent device performance.[76,288]

OSC single crystals can be grown from either vapor or solution phase. Fabricating patterned single-crystal arrays over large areas is necessary for practical applications of single crystal devices.[76] This can be achieved through patterning the nucleation and crystal growth regions for selective growth through chemical contrast[289] or surface roughness (Figure 16b–d).[76,290]

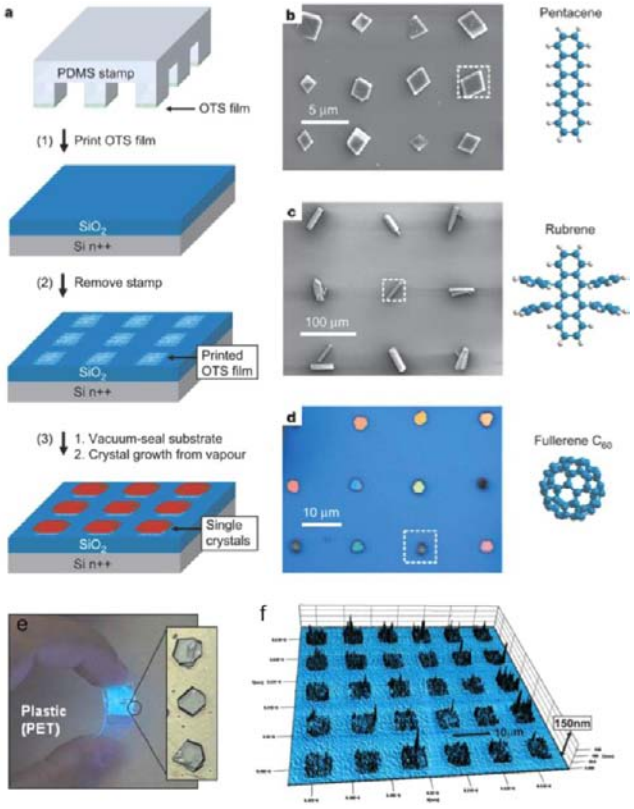

Figure 16. Schematic outline of the procedure used to grow organic single crystals on substrates that have been patterned by microcontact printing. (a–e) Adapted with permission from ref 76. Copyright 2006 Nature Publishing Group. (f) Reproduced with permission from ref 291. Copyright 2007 WILEY-VCH Verlag GmbH & Co.

Compared with solution phase processing, physical vapor transport[292−294] is limited in that (1) often high temperature for sublimation is required; (2) its low deposition rate is not amenable for high-throughput fabrication on a large area; (3) few processing parameters can be tuned to control the crystal morphology. With an increasing number of soluble OSCs reported, several solution-processing methods have been developed for making single crystal devices, primarily by drop-casting based methods. Single-crystalline TIPS-PEN microribbons were prepared by a solvent-exchange method combined with drop casting.[295] Micron-sized C_8–BTBT single-crystal needles were formed by solvent vapor annealing of spin-coated polycrystalline films.[296] However, these methods do not impart orientational control with the single-crystals obtained. Crystal orientation can be guided by controlling the concentration gradient generated during solvent evaporation.

A droplet-pinned crystallization method (DPC) was reported recently, which produces aligned single-crystalline ribbons over a large area.[74] Nucleation density is tuned by varying the solution concentration (Figure 17), and a steady receding contact line is facilitated by pinning the droplet using a small

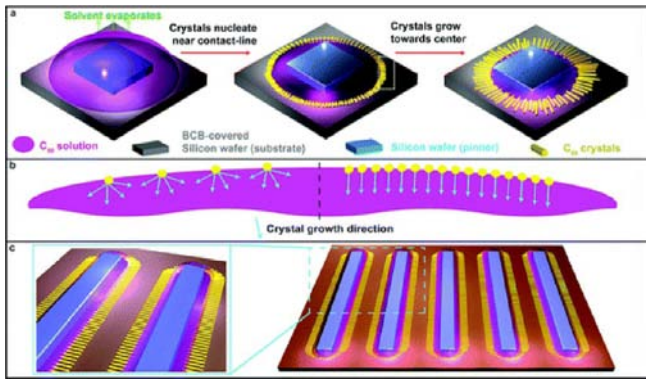

Figure 17. Schematic representations of the DPC method. (a) An organic semiconductor droplet pinned by a silicon wafer. As the solvent evaporates slowly, the crystals of the organic semiconductors nucleate near the contact line of the droplet. Subsequently, the nuclei grow along the receding direction (toward the center) of the droplet. (b) A magnified view of a white-marked area in panel a, highlighting the contact line where a high nucleation density (right side) leads to unidirectional crystallization along the receding direction of the droplet, while a low nucleation density (left side) results in nondirectional crystallization. (c) DPC can be scaled up by using multiple pinners with larger sizes. Elongation of the pinner leads to unidirectional parallel alignment of the crystals. Reproduced with permission from ref 74. Copyright 2012 from American Chemical Society.

piece of silicon wafer (Figure 17a,c). With this method, well-aligned C_{60} single-crystal needles and ribbons were fabricated, showing electron mobility as high as 11 $cm^2/(V\ s)$. At the time of publication, this observed mobility is 8-fold higher than the maximum reported mobility for solution-grown n-channel organic materials (1.5 $cm^2/(V\ s)$) and is 2-fold higher than the highest mobility of any n-channel organic material (6 $cm^2/(V\ s)$).[79] High device performance by the DPC method is partially attributed to an intimate crystal interface with the dielectric during *in situ* growth of single crystals on the device substrates.

The authors also showed that DPC is scalable to a 100 mm wafer substrate, with around 50% of the wafer surface covered by aligned crystals. The authors further demonstrated the advantage of DPC by positioning both p- and n-channel OSCs on a common substrate to fabricate complementary circuits.[88] One of the drawbacks of DPC, however, is the relatively long processing time, which may limit its applicability to high-throughput industrial manufacturing.

For patterning solution grown single-crystals, nucleation control is necessary to tune the nucleation density and spatial distribution on the substrates. It is desirable to have a single nucleation event at each designated location on the substrate. However, this goal is challenging to achieve given the stochastic nature of nucleation. Due to this reason, solution processing methods aiming to obtain patterned, single-crystal arrays often yield a high proportion of polycrystalline domains.[4,247] Recently, patterned single crystals of 3,9-bis(4-ethylphenyl)-peri-xanthenoxanthene (C2Ph-PXX) were prepared with high yield using patterned nucleation regions through chemical contrast (see Figure 18).[72] Smaller solution volume resulted in a faster solvent evaporation, and therefore supersaturation was

dx.doi.org/10.1021/ja400881n | J. Am. Chem. Soc. 2013, 135, 6724−6746

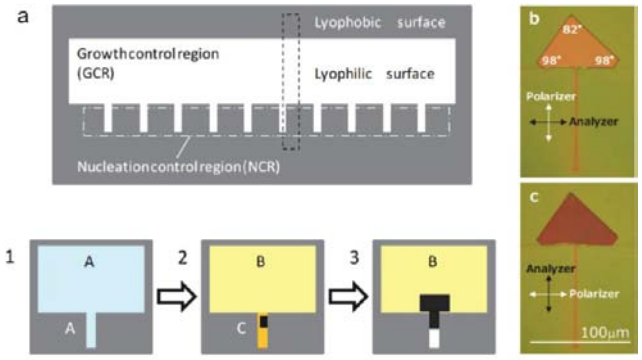

Figure 18. (a) Original micropattern with nucleation control region (NCR) and growth control region (GCR) and schematic diagram of growth model. (b and c) Crossed Nicols polarized micrographs of the same thin film. The thin film has a typical pentagon shape with characteristic angles of 82° and 98°. Reproduced with permission from ref 72. Copyright 2012 WILEY-VCH Verlag GmbH & Co.

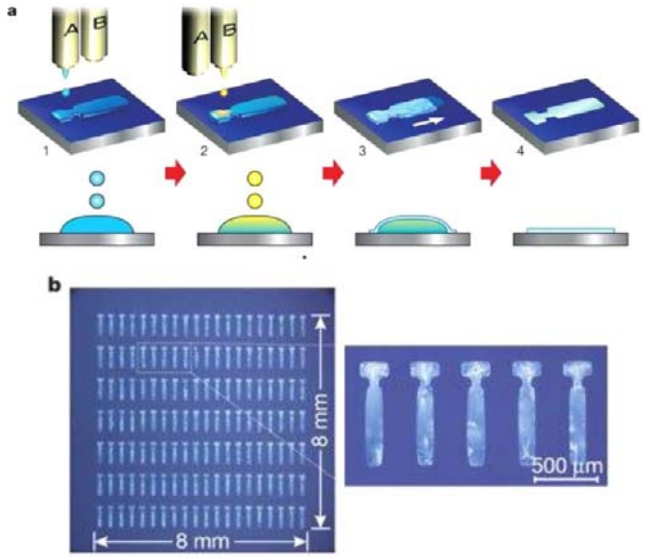

Figure 19. Inkjet printing of organic single-crystal thin films. (a) Schematic of the process. Antisolvent ink (A) is first inkjet-printed (step 1), and then solution ink (B) is overprinted sequentially to form intermixed droplets confined to a predefined area (step 2). Semiconducting thin films grow at liquid−air interfaces of the droplet (step 3), before the solvent fully evaporates (step 4). (b) Micrographs of a 20 × 7 array of inkjet-printed C8-BTBT single-crystal thin films. Reproduced with permission from ref 4. Copyright 2011 Nature Publishing Group.

first achieved in the small regions where nucleation was induced. The solvent evaporation rate was further regulated by controlling the solvent vapor pressure, which is important for maintaining steady crystal growth and obtaining reproducible results. By narrowing the width of the nucleation control region to 5 μm, a preferred orientation of the single crystals was observed. However, the degree of crystal alignment is low. As the authors noted, alignment of the crystal orientation is extremely important due to the anisotropic nature of the field-effect mobility.

So far, most of the solution grown single crystals were fabricated using drop casting based methods in which solvent evaporation often takes hours. Slow crystal growth is considered necessary for achieving high purity and low defect density, and thus high performance. Attaining single crystals directly through solution printing remains challenging, due to rapid solvent evaporation and fluid flow instabilities during the printing process. The use of solution printing techniques for the fabrication of patterned single-crystals has not been demonstrated until recently. A novel use of inkjet printing combined with antisolvent crystallization was reported for making single crystal arrays of $2C_8$−BTBT.[4] The schematic of the method is shown in Figure 19. Antisolvent (in this case, *N*,*N*-dimethylformamide) was dropped onto hydrophilic regions predefined via surface patterning, then subsequently overprinted with solution droplets of C_8-BTBT in 1,2-dichlorobenzene. The thin film transistors thus fabricated yielded hole carrier mobility as high as 31.3 $cm^2/(V\ s)$. Nonetheless, a few drawbacks with this method are yet to be addressed. The probability of obtaining single crystals of C_8-BTBT was reported to be approximately 50%, which leaves room for improving the method for nucleation control. Moreover, this method yields a wide crystal orientation distribution. The lack of crystal alignment mechanism may be partially responsible for the large variation in charge carrier mobility.

Alignment of single crystals over a large area during solution deposition can be achieved via multiple means. The most commonly used method is the use of concentration or temperature gradients generated during solvent evaporation, as mentioned before. Novel methods such as flow-induced alignment have been demonstrated as well.[297−299] Figure 20 shows such an example, where the flow field was utilized for aligning OSC microwires. In this study, a filtration-and-transfer (FAT) method was reported that allows for efficient alignment of organic wires with controllable density as well as the formation of multiple, discrete microwire patterns aligned in different directions.[85] Briefly, OSC microwires were aligned by fluid flow through a mask in a modified, simple vacuum filtration setup. Individual single-crystalline PTCDI microwire-OFETs showed charge carrier mobilities up to 1.4 $cm^2/(V\ s)$, among the highest solution-processed n-channel organic semiconducting wire devices, while a random network of high-density microwire-OFETs only exhibited mobilities around 0.14 $cm^2/(V\ s)$.[85] This approach has some limitations. The introduction and removal of polydimethylsiloxane (PDMS) mask and anodic aluminum oxide (AAO) template make the fabrication process complicated and will likely limit its practical applications. A variety of alignment methods have been surveyed.[264,300]

Examples discussed above illustrate both the opportunities and challenges in fabricating aligned, patterned, single-crystal arrays using a process compatible with large-scale, high-throughput industrial productions. Various solution coating/printing methods, such as slot-die coating, solution shearing, and inkjet printing are promising candidates for achieving this goal. To successfully develop a solution processing technique for making patterned, aligned single crystal arrays, the following elements are essential: control over nucleation locations and nuclei density, low-defect crystal growth at high coating/printing speed, a mechanism for directing crystal orientation (e.g., controlled supersaturation gradient or patterned flow field), and a method for achieving patterning with high resolution.

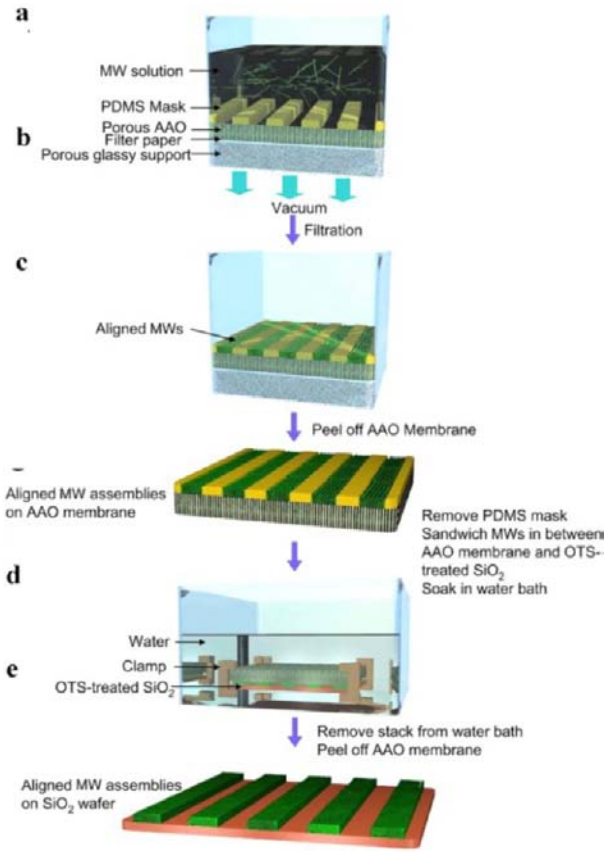

Figure 20. Schematic diagram for FAT alignment of organic microwires (MWs). (a) FAT alignment apparatus loaded with the MW dispersion. A PDMS mask with open-stripe patterns is placed on a porous AAO membrane. The microwire dispersion is filtered by applying vacuum. (b) MW assemblies reside exclusively inside the stripe patterns of the PDMS mask after filtration. (c) AAO membrane covered with patterned MWs inside the PDMS mask. (d) Illustration for the transfer of the aligned MW patterns from an AAO membrane to a desired wafer substrate in aqueous medium. MWs selectively adhere to the OTS-treated SiO_2 as water diffuses through the pores of the AAO membrane. (e) Aligned MWs were transferred onto the wafer. Reproduced with permission from ref 85. Copyright 2009 National Academy of Sciences, U.S.A.

4. COMPUTER AIDED DESIGN OF ORGANIC SEMICONDUCTORS: A THEORETICAL APPROACH

The search for high mobility organic materials for optoelectronic applications has primarily been done through the following progression: synthesis, characterization, application, and *post facto* computational studies to better understand the structure−property-performance relationship. In many cases, strategies to design new materials are based on results of known materials and progress moves at the pace of synthesis and fabrication in a trial and error methodology. Ultimately, a theory-guided material design strategy is necessary for truly rational design of materials. However, this remains challenging as a better understanding of charge transport processes and the related theory to precisely predict charge carrier mobility are still needed. An alternative approach would be *a priori* screening of potential materials candidates computationally to select the most promising candidates, in collaboration with synthetic chemists to assess synthetic viability, and then target the best candidate(s) for application, thus potentially reducing time-consuming experiments and costs.

In the case of organic transistors, theoretical modeling has been used to understand structure property relationships for many years. However, *in silico* design of OSCs remains challenging. First, in order to predict *de novo* the magnitude and anisotropy of charge transport, the crystal structure must be calculated computationally, which was noted as the major bottleneck for the application of *in silico* screening to organic crystalline semiconducting materials.[95] Until recently, this parameter could only be reasonably computationally obtained for small organic rigid molecules, where large conjugated heteroacenes are precluded.[301,302] However, even if the precise crystal structure is known, accurate calculation of charge carrier mobility is still difficult as current theory can not fully account for all processes taking place in the device. Finally, thin film molecular packing may be different from bulk structure while thin film morphology is highly dependent on substrate surface properties as well as OSC molecular structures.

Despite the above-described challenges, there have been some success with *in silico* design in organic transistors through screening of derivatives. One such example resulted in the successful discovery of a small molecule semiconductor while another resulted in a high mobility polymer semiconductor. The process began with inspiration from work by Yamamoto and Takimiya on a dinaphthothienothiophene (DNTT, **1**) that showed exceptional hole mobility above 1 $cm^2/(V\ s)$ and air stability.[121,303] Using a combined quantum-mechanical and molecular mechanics computational approach, the Aspuru-Guzik group screened novel thienothiophene derivatives from fused aromatics (**2**−**8**), then narrowed the search by eliminating candidates with high reorganization energies. It is further narrowed to only one candidate DATT (**2**) (Figure 21)

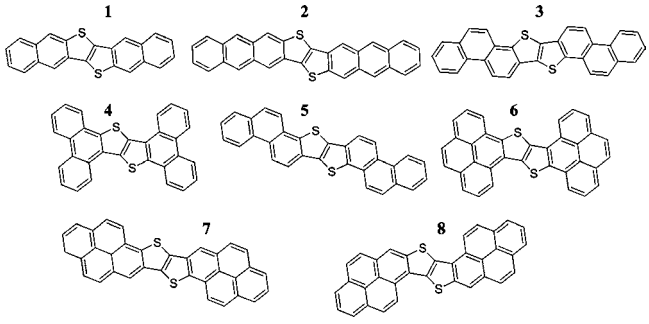

Figure 21. The structures of the seven heteroacenes generated *in silico* based on DNTT that were computationally characterized as potential high-performance organic semiconductors.

after performing crystal structure optimization and evaluating the charge transport parameters to calculate mobility. It should be mentioned that DNTT (**1**) was used as a benchmark for these computational studies, and it was found to be in acceptable agreement across a series of parameters with experiment, thereby providing confidence in this methodology. The Bao group then synthesized this derivative and evaluated its performance in a single-crystal OFET device, which resulted in a saturation region hole mobility of 12.3 $cm^2/(V\ s)$ and a linear region mobility of 16 $cm^2/(V\ s)$.

A similar methodology was recently applied to polymeric materials. To achieve this, four representative repeat units of the DPP-based polymers were modeled (see Figure 22).[5] After modeling each repeat unit and obtaining an optimized $\pi-\pi$ stacking distance, they calculated the theoretical drift mobility

dx.doi.org/10.1021/ja400881n | J. Am. Chem. Soc. 2013, 135, 6724−6746

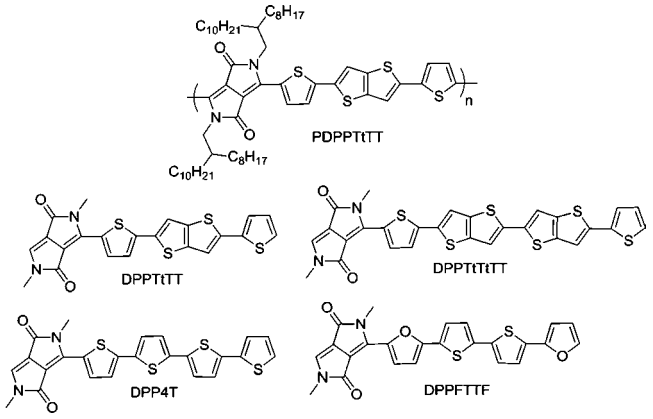

Figure 22. Structures of the synthesized polymer and the D−A model monomers for computational analysis.

of each representative derivative. Of the four derivatives studied, DPPTtTT showed the highest potential drift mobility, which gave the authors confidence that this could be a high mobility p-type polymer. Each of the representative repeating units had previously been synthesized into polymers, which showed good correlation with their calculated drift mobilities, except DPPTtTT. Devices previously fabricated from DPPTtTT had shown inferior mobility that was attributed to low molecular weight. The authors achieved much higher molecular weight polymers than previously reported, and optimized the FET devices. They found the highest mobility to be 10.5 $cm^2/(V\ s)$ with high on/off ratios, a factor of 5 times greater than their calculated mobility and more than an order of magnitude increase as compared to the lower molecular weight version. The process of utilizing computer simulation to evaluate potential high mobility materials has thus resulted in a small molecule and polymer, both of which have achieved record hole mobilities.

These papers on the computational discovery of high mobility OSCs where the computer aided design before synthesis and application took place should be cause for great hope in continuously discovering new high performing organic materials for optoelectronic applications. *In silico* evaluation of novel semiconducting crystalline materials and polymers can take place, thus directing synthetic chemists toward the highest performing derivatives. The computational chemist will not only be asked "Why does this material work?", but can now also answer "Which derivative do I expect the best outcome, even before synthesis begins?" A requirement of this type of methodology is productive collaborative relationships between computational chemists, synthetic chemists, and device engineers. *In silico* screening can also generate libraries of hundreds of thousands of potential candidates, but the computer is not aware of synthetic viability, nor is the computer able to assess the plethora of variables during device fabrication. It would be a wonder and the ultimate goal to have a computer create a library of synthetically viable materials candidates, and evaluate their performance and how that performance could be manipulated through fabrication techniques and processes.

5. SUMMARY AND OUTLOOK

The development of OSCs for OFETs is advancing rapidly. Molecular design has led to remarkable advances in the creation of various high-performance OSCs. An integrated design approach combining molecular design and process engineering through the control of film morphology and molecular packing of OSCs has enabled a better fundamental understanding of charge transport in organic materials and pushed OFETs ever closer to practical applications. *In silico* screening has demonstrated its initial success and is the ultimate approach for designing future high performance OSCs. A great deal of research efforts are still needed; the synergy of chemical design, process engineering and theoretical calculations bodes well for a bright future in OFETs.

On the other hand, there are a few challenges the research community has to overcome before OFETs can take off for practical applications. Organic circuits are generally featured as low cost electronics, even though there is still lack of a comprehensive and accessible analysis of cost-structures of OFET devices for various applications. From the aspect of synthetic chemistry, there are a few cost drivers, namely, reaction steps and yields, reagents and solvents, as well as purification approaches. To make a positive contribution in the cost reduction, it is important to design a cost-effective (less reaction steps, high reaction yields, as well as environmental-friendly reagents and solvents) and scalable (capable of scaling from miligrams to hundreds of grams) synthetic route, as well as to adopt a simple and reliable purification process. Currently, sophisticated purification techniques (e.g., recycling gel permeation chromatography) are required to obtain high purity materials, crucial for high performance and reproducibility in devices. This is a trade-off we have to manage. As far as printing processing is concerned, use of chlorinated solvents is strongly disfavored. Not only does it increase the cost, but it also poses an adverse environmental impact. Unfortunately, the majority high performance OFET materials are currently processed from chlorinated solvents. It is thus important for chemists to develop OFET materials that can be processed from nonchlorinated solvents, while retaining high performance.

Some other issues for OFETs include (1) the long-term storage and operation stability of the devices, (2) the reliability and reproducibility of the devices, (3) and the patterning and integration of OFETs in integrated circuits. To create solutions for these challenges, not only are OSC design and processing important, but the advancement of dielectric and encapsulation materials is also crucial. In addition, environmental assessment of OSCs is needed, since they are aromatic compounds and likely to be carcinogens. This is especially critical, if OFETs are ever used in disposable devices.

AUTHOR INFORMATION

Corresponding Author

zbao@stanford.edu

Notes

The authors declare no competing financial interest.

ACKNOWLEDGMENTS

This work is supported by the Center for Advanced Molecular Photovoltaics, made by King Abdullah University of Science and Technology, the Department of Energy, Laboratory Directed Research and Development funding, under contract DE-AC02-76SF00515, Air Force Office of Scientific Research (FA9550-12-1-01906), National Science Foundation (DMR-1006989) and DARPA Qube Program. We also acknowledge the Camille and Henry Dreyfus Postdoctoral Program in

Environmental Chemistry, and the support from the Global Climate and Energy Program at Stanford.

REFERENCES

(1) Mallik, A. B.; Locklin, J.; Mannsfeld, S. C. B.; Reese, C.; Roberts, M. E.; Senatore, M. L.; Zi, H.; Bao, Z. In *Organic Field-Effect Transistors*; Zhenan, B., Locklin, J. J., Eds.; CRC Press: Boca Raton, FL, 2007, p 159−228.
(2) Wang, C.; Dong, H.; Hu, W.; Liu, Y.; Zhu, D. *Chem. Rev.* **2011**, *112*, 2208−2267.
(3) Amin, A. Y.; Khassanov, A.; Reuter, K.; Meyer-Friedrichsen, T.; Halik, M. *J. Am. Chem. Soc.* **2012**, *134*, 16548−16550.
(4) Minemawari, H.; Yamada, T.; Matsui, H.; Tsutsumi, J. y.; Haas, S.; Chiba, R.; Kumai, R.; Hasegawa, T. *Nature* **2011**, *475*, 364−367.
(5) Li, J.; Zhao, Y.; Tan, H. S.; Guo, Y.; Di, C.-A.; Yu, G.; Liu, Y.; Lin, M.; Lim, S. H.; Zhou, Y.; Su, H.; Ong, B. S. *Sci. Rep.* **2012**, *2*, 754.
(6) Menard, E.; Podzorov, V.; Hur, S. H.; Gaur, A.; Gershenson, M. E.; Rogers, J. A. *Adv. Mater.* **2004**, *16*, 2097−2101.
(7) Jurchescu, O. D.; Popinciuc, M.; van Wees, B. J.; Palstra, T. T. M. *Adv. Mater.* **2007**, *19*, 688−692.
(8) Reese, C.; Bao, Z. *Adv. Mater.* **2007**, *19*, 4535−4538.
(9) Sundar, V. C.; Zaumseil, J.; Podzorov, V.; Menard, E.; Willett, R. L.; Someya, T.; Gershenson, M. E.; Rogers, J. A. *Science* **2004**, *303*, 1644−1646.
(10) Tsumura, A.; Koezuka, H.; Ando, T. *Appl. Phys. Lett.* **1986**, *49*, 1210−1212.
(11) Madru, M.; Guillaud, G.; Sadoun, M. A.; Maitrot, M.; Clarisse, C.; Contellec, M. L.; André, J. J.; Simon, J. *Chem. Phys. Lett.* **1987**, *142*, 103−105.
(12) Garnier, F.; Hajlaoui, R.; Yassar, A.; Srivastava, P. *Science* **1994**, *265*, 1684−1686.
(13) Bao, Z.; Dodabalapur, A.; Lovinger, A. J. *Appl. Phys. Lett.* **1996**, *69*, 4108−4110.
(14) Bao, Z.; Feng, Y.; Dodabalapur, A.; Raju, V. R.; Lovinger, A. J. *Chem. Mater.* **1997**, *9*, 1299−1301.
(15) Sirringhaus, H.; Kawase, T.; Friend, R. H.; Shimoda, T.; Inbasekaran, M.; Wu, W.; Woo, E. P. *Science* **2000**, *290*, 2123−2126.
(16) Bao, Z.; A. Rogers, J.; E. Katz, H. *J. Mater. Chem.* **1999**, *9*, 1895−1904.
(17) Rogers, J. A.; Bao, Z.; Makhija, A.; Braun, P. *Adv. Mater.* **1999**, *11*, 741−745.
(18) Dimitrakopoulos, C. D.; Malenfant, P. R. L. *Adv. Mater.* **2002**, *14*, 99−117.
(19) Mcculloch, I. *Nat. Mater.* **2005**, *4*, 583−584.
(20) Stingelin-Stutzmann, N.; Smits, E.; Wondergem, H.; Tanase, C.; Blom, P.; Smith, P.; de Leeuw, D. *Nat. Mater.* **2005**, *4*, 601−606.
(21) Forrest, S. R. *Nature* **2004**, *428*, 911−918.
(22) Kim, C.; Burrows, P. E.; Forrest, S. R. *Science* **2000**, *288*, 831−833.
(23) Meng, H.; Zheng, J.; Lovinger, A. J.; Wang, B.-C.; Van Patten, P. G.; Bao, Z. *Chem. Mater.* **2003**, *15*, 1778−1787.
(24) Mushrush, M.; Facchetti, A.; Lefenfeld, M.; Katz, H. E.; Marks, T. J. *J. Am. Chem. Soc.* **2003**, *125*, 9414−9423.
(25) Bao, Z.; Lovinger, A. J.; Dodabalapur, A. *Appl. Phys. Lett.* **1996**, *69*, 3066−3068.
(26) Liu, S.; Wang, W. M.; Briseno, A. L.; Mannsfeld, S. C. B.; Bao, Z. *Adv. Mater.* **2009**, *21*, 1217−1232.
(27) Afzali, A.; Dimitrakopoulos, C. D.; Breen, T. L. *J. Am. Chem. Soc.* **2002**, *124*, 8812−8813.
(28) Yen-Yi, L.; Gundlach, D. I.; Nelson, S. F.; Jackson, T. N. *IEEE Trans. Electron Devices* **1997**, *44*, 1325−1331.
(29) Yang, H.; Shin, T. J.; Ling, M.-M.; Cho, K.; Ryu, C. Y.; Bao, Z. *J. Am. Chem. Soc.* **2005**, *127*, 11542−11543.
(30) Zhang, X.-H.; Tiwari, S. P.; Kim, S.-J.; Kippelen, B. *Appl. Phys. Lett.* **2009**, *95*, 223302−223303.
(31) Roberts, M. E.; Mannsfeld, S. C. B.; Queraltó, N.; Reese, C.; Locklin, J.; Knoll, W.; Bao, Z. *Proc. Natl. Acad. Sci. U.S.A.* **2008**, *105*, 12134−12139.
(32) Jurchescu, O. D.; Baas, J.; Palstra, T. T. M. *Appl. Phys. Lett.* **2004**, *84*, 3061−3063.
(33) Kane, M. G.; Campi, J.; Hammond, M. S.; Cuomo, F. P.; Greening, B.; Sheraw, C. D.; Nichols, J. A.; Gundlach, D. J.; Huang, J. R.; Kuo, C. C.; Jia, L.; Klauk, H.; Jackson, T. N. *IEEE Electron Device Lett.* **2000**, *21*, 534−536.
(34) Gelinck, G. H.; Huitema, H. E. A.; van Veenendaal, E.; Cantatore, E.; Schrijnemakers, L.; van der Putten, J. B. P. H.; Geuns, T. C. T.; Beenhakkers, M.; Giesbers, J. B.; Huisman, B.-H.; Meijer, E. J.; Benito, E. M.; Touwslager, F. J.; Marsman, A. W.; van Rens, B. J. E.; de Leeuw, D. M. *Nat. Mater.* **2004**, *3*, 106−110.
(35) Rogers, J. A.; Bao, Z.; Baldwin, K.; Dodabalapur, A.; Crone, B.; Raju, V. R.; Kuck, V.; Katz, H.; Amundson, K.; Ewing, J.; Drzaic, P. *Proc. Natl. Acad. Sci. U.S.A.* **2001**, *98*, 4835−4840.
(36) Kang, M. J.; Doi, I.; Mori, H.; Miyazaki, E.; Takimiya, K.; Ikeda, M.; Kuwabara, H. *Adv. Mater.* **2011**, *23*, 1222−1225.
(37) Kim, S. H.; Yoon, W. M.; Jang, M.; Yang, H.; Park, J.-J.; Park, C. E. *J. Mater. Chem.* **2012**, *22*, 7731−7738.
(38) Feili, D.; Schuettler, M.; Doerge, T.; Kammer, S.; Stieglitz, T. *Sens. Actuators, A* **2005**, *120*, 101−109.
(39) Katz, H. E. *Chem. Mater.* **2004**, *16*, 4748−4756.
(40) Zhang, L.; Di, C.-a.; Yu, G.; Liu, Y. *J. Mater. Chem.* **2010**, *20*, 7059−7073.
(41) Brown, A. R.; Jarrett, C. P.; de Leeuw, D. M.; Matters, M. *Synth. Met.* **1997**, *88*, 37−55.
(42) Payne, M. M.; Parkin, S. R.; Anthony, J. E.; Kuo, C.-C.; Jackson, T. N. *J. Am. Chem. Soc.* **2005**, *127*, 4986−4987.
(43) Allard, S.; Forster, M.; Souharce, B.; Thiem, H.; Scherf, U. *Angew. Chem., Int. Ed.* **2008**, *47*, 4070−4098.
(44) Gao, P.; Beckmann, D.; Tsao, H. N.; Feng, X.; Enkelmann, V.; Baumgarten, M.; Pisula, W.; Müllen, K. *Adv. Mater.* **2009**, *21*, 213−216.
(45) Gao, P.; Beckmann, D.; Tsao, H. N.; Feng, X.; Enkelmann, V.; Pisula, W.; Mullen, K. *Chem. Commun.* **2008**, 1548−1550.
(46) Garnier, F.; Hajlaoui, R.; El Kassmi, A.; Horowitz, G.; Laigre, L.; Porzio, W.; Armanini, M.; Provasoli, F. *Chem. Mater.* **1998**, *10*, 3334−3339.
(47) Katz, H. E.; Lovinger, A. J. *Nature* **2000**, *404*, 478.
(48) Yamada, H.; Ohashi, C.; Aotake, T.; Katsuta, S.; Honsho, Y.; Kawano, H.; Okujima, T.; Uno, H.; Ono, N.; Seki, S.; Nakayama, K.-i. *Chem. Commun.* **2012**, *48*, 11136−11138.
(49) Yamada, H.; Okujima, T.; Ono, N. *Chem. Commun.* **2008**, *0*, 2957−2974.
(50) Herwig, P. T.; Müllen, K. *Adv. Mater.* **1999**, *11*, 480−483.
(51) Murphy, A. R.; Fréchet, J. M. J.; Chang, P.; Lee, J.; Subramanian, V. *J. Am. Chem. Soc.* **2004**, *126*, 1596−1597.
(52) Weidkamp, K. P.; Afzali, A.; Tromp, R. M.; Hamers, R. J. *J. Am. Chem. Soc.* **2004**, *126*, 12740−12741.
(53) Afzali, A.; Dimitrakopoulos, C. D.; Graham, T. O. *Adv. Mater.* **2003**, *15*, 2066−2069.
(54) Ebata, H.; Izawa, T.; Miyazaki, E.; Takimiya, K.; Ikeda, M.; Kuwabara, H.; Yui, T. *J. Am. Chem. Soc.* **2007**, *129*, 15732−15733.
(55) Mitsui, C.; Soeda, J.; Miwa, K.; Tsuji, H.; Takeya, J.; Nakamura, E. *J. Am. Chem. Soc.* **2012**, *134*, 5448−5451.
(56) Giri, G.; Verploegen, E.; Mannsfeld, S. C. B.; Atahan-Evrenk, S.; Kim, D. H.; Lee, S. Y.; Becerril, H. A.; Aspuru-Guzik, A.; Toney, M. F.; Bao, Z. A. *Nature* **2011**, *480*, 504−508.
(57) Uemura, T.; Hirose, Y.; Uno, M.; Takimiya, K.; Takeya, J. *Appl. Phys. Express* **2009**, *2*, 111501.
(58) Sirringhaus, H.; Tessler, N.; Friend, R. H. *Science* **1998**, *280*, 1741−1744.
(59) Wang, G.; Swensen, J.; Moses, D.; Heeger, A. J. *J. Appl. Phys.* **2003**, *93*, 6137−6141.
(60) Ong, B. S.; Wu, Y.; Liu, P.; Gardner, S. *J. Am. Chem. Soc.* **2004**, *126*, 3378−3379.
(61) McCulloch, I.; Heeney, M.; Bailey, C.; Genevicius, K.; MacDonald, I.; Shkunov, M.; Sparrowe, D.; Tierney, S.; Wagner, R.; Zhang, W.; Chabinyc, M. L.; Kline, R. J.; McGehee, M. D.; Toney, M. F. *Nat. Mater.* **2006**, *5*, 328−333.

(62) Fong, H. H.; Pozdin, V. A.; Amassian, A.; Malliaras, G. G.; Smilgies, D.-M.; He, M.; Gasper, S.; Zhang, F.; Sorensen, M. *J. Am. Chem. Soc.* **2008**, *130*, 13202−13203.
(63) Osaka, I.; Shinamura, S.; Abe, T.; Takimiya, K. *J. Mater. Chem. C.* **2013**, 1297−1304.
(64) Tsao, H. N.; Cho, D. M.; Park, I.; Hansen, M. R.; Mavrinskiy, A.; Yoon, D. Y.; Graf, R.; Pisula, W.; Spiess, H. W.; Müllen, K. *J. Am. Chem. Soc.* **2011**, *133*, 2605−2612.
(65) Sonar, P.; Singh, S. P.; Li, Y.; Soh, M. S.; Dodabalapur, A. *Adv. Mater.* **2010**, *22*, 5409−5413.
(66) Nielsen, C. B.; Turbiez, M.; McCulloch, I. *Adv. Mater.* **2012**, n/a−n/a.
(67) Lei, T.; Cao, Y.; Fan, Y.; Liu, C.-J.; Yuan, S.-C.; Pei, J. *J. Am. Chem. Soc.* **2011**, *133*, 6099−6101.
(68) Lei, T.; Cao, Y.; Zhou, X.; Peng, Y.; Bian, J.; Pei, J. *Chem. Mater.* **2012**, *24*, 1762−1770.
(69) Mei, J.; Kim, D. H.; Ayzner, A. L.; Toney, M. F.; Bao, Z. *J. Am. Chem. Soc.* **2011**, *133*, 20130−20133.
(70) Nielsen, C. B.; Turbiez, M.; McCulloch, I. *Adv. Mater.* **2013**, *25*, 1859−1880.
(71) Lei, T.; Dou, J.-H.; Pei, J. *Adv. Mater.* **2012**, *24*, 6457−6461.
(72) Goto, O.; Tomiya, S.; Murakami, Y.; Shinozaki, A.; Toda, A.; Kasahara, J.; Hobara, D. *Adv. Mater.* **2012**, *24*, 1117−1122.
(73) Islam, M. M.; Pola, S.; Tao, Y.-T. *Chem. Commun.* **2011**, *47*, 6356−6358.
(74) Li, H.; Tee, B. C. K.; Cha, J. J.; Cui, Y.; Chung, J. W.; Lee, S. Y.; Bao, Z. *J. Am. Chem. Soc.* **2012**, *134*, 2760−2765.
(75) Briseno, A. L.; Tseng, R. J.; Ling, M. M.; Falcao, E. H. L.; Yang, Y.; Wudl, F.; Bao, Z. *Adv. Mater.* **2006**, *18*, 2320−2324.
(76) Briseno, A. L.; Mannsfeld, S. C. B.; Ling, M. M.; Liu, S.; Tseng, R. J.; Reese, C.; Roberts, M. E.; Yang, Y.; Wudl, F.; Bao, Z. *Nature* **2006**, *444*, 913−917.
(77) Kim, Y.-H.; Yoo, B.; Anthony, J. E.; Park, S. K. *Adv. Mater.* **2012**, *24*, 497−502.
(78) Tang, Q.; Jiang, L.; Tong, Y.; Li, H.; Liu, Y.; Wang, Z.; Hu, W.; Liu, Y.; Zhu, D. *Adv. Mater.* **2008**, *20*, 2947−2951.
(79) Anthopoulos, T. D.; Singh, B.; Marjanovic, N.; Sariciftci, N. S.; Ramil, A. M.; Sitter, H.; Colle, M.; Leeuw, D. M. d. *Appl. Phys. Lett.* **2006**, *89*, 213504.
(80) Podzorov, V.; Menard, E.; Borissov, A.; Kiryukhin, V.; Rogers, J. A.; Gershenson, M. E. *Phys. Rev. Lett.* **2004**, *93*, 086602.
(81) Reese, C.; Chung, W.-J.; Ling, M.-m.; Roberts, M.; Bao, Z. *Appl. Phys. Lett.* **2006**, *89*, 202108.
(82) Takeya, J.; Yamagishi, M.; Tominari, Y.; Hirahara, R.; Nakazawa, Y.; Nishikawa, T.; Kawase, T.; Shimoda, T.; Ogawa, S. *Appl. Phys. Lett.* **2007**, *90*, 102120−102123.
(83) Mannsfeld, S. C. B.; Tee, B. C. K.; Stoltenberg, R. M.; Chen, C. V. H. H.; Barman, S.; Muir, B. V. O.; Sokolov, A. N.; Reese, C.; Bao, Z. *Nat. Mater.* **2010**, *9*, 859−864.
(84) Kumatani, A.; Liu, C.; Li, Y.; Darmawan, P.; Takimiya, K.; Minari, T.; Tsukagoshi, K. *Sci. Rep.* **2012**, *2*, 393.
(85) Oh, J. H.; Lee, H. W.; Mannsfeld, S.; Stoltenberg, R. M.; Jung, E.; Jin, Y. W.; Kim, J. M.; Yoo, J.-B.; Bao, Z. *Proc. Natl. Acad. Sci. U.S.A.* **2009**, *106*, 6065−6070.
(86) Sheraw, C. D.; Jackson, T. N.; Eaton, D. L.; Anthony, J. E. *Adv. Mater.* **2003**, *15*, 2009−2011.
(87) Park, S. K.; Jackson, T. N.; Anthony, J. E.; Mourey, D. A. *Appl. Phys. Lett.* **2007**, *91*, 063514.
(88) Li, H.; Tee, B. C. K.; Giri, G.; Chung, J. W.; Lee, S. Y.; Bao, Z. *Adv. Mater.* **2012**, *24*, 2588−2591.
(89) Sokolov, A. N.; Atahan-Evrenk, S.; Mondal, R.; Akkerman, H. B.; Sanchez-Carrera, R. S.; Granados-Focil, S.; Schrier, J.; Mannsfeld, S. C. B.; Zoombelt, A. P.; Bao, Z.; Aspuru-Guzik, A. *Nat. Commun.* **2011**, *2*, 437.
(90) Liu, C.; Minari, T.; Lu, X.; Kumatani, A.; Takimiya, K.; Tsukagoshi, K. *Adv. Mater.* **2011**, *23*, 523−+.
(91) Hasegawa, T.; Takeya, J. *Sci. Technol. Adv. Mater.* **2009**, *10*, 024314.
(92) Usta, H.; Facchetti, A.; Marks, T. J. *Acc. Chem. Res.* **2011**, *44*, 501−510.
(93) Yuen, J. D.; Wudl, F. *Energy Environ. Sci.* **2013**, 392−406.
(94) Marcus, R. A. *Annu. Rev. Phys. Chem.* **1964**, *15*, 155−196.
(95) Wang, L.; Nan, G.; Yang, X.; Peng, Q.; Li, Q.; Shuai, Z. *Chem. Soc. Rev.* **2010**, *39*, 423−434.
(96) Coropceanu, V.; Cornil, J.; da Silva, D. A.; Olivier, Y.; Silbey, R.; Bredas, J. L. *Chem. Rev.* **2007**, *107*, 926−952.
(97) Aleshin, A. N.; Lee, J. Y.; Chu, S. W.; Kim, J. S.; Park, Y. W. *Appl. Phys. Lett.* **2004**, *84*, 5383−5385.
(98) Boer, R. W. I. d.; Klapwijk, T. M.; Morpurgo, A. F. *Appl. Phys. Lett.* **2003**, *83*, 4345−4347.
(99) Takeyama, Y.; Ono, S.; Matsumoto, Y. *Appl. Phys. Lett.* **2012**, *101*, 083303.
(100) Mondal, R.; Shah, B. K.; Neckers, D. C. *J. Am. Chem. Soc.* **2006**, *128*, 9612−9613.
(101) Watanabe, M.; Chang, Y. J.; Liu, S.-W.; Chao, T.-H.; Goto, K.; IslamMd, M.; Yuan, C.-H.; Tao, Y.-T.; Shinmyozu, T.; Chow, T. J. *Nat. Chem.* **2012**, *4*, 574−578.
(102) Zade, S. S.; Bendikov, M. *Angew. Chem., Int. Ed.* **2010**, *49*, 4012−4015.
(103) Tönshoff, C.; Bettinger, H. F. *Angew. Chem., Int. Ed.* **2010**, *49*, 4125−4128.
(104) Appleton, A. L.; Barlow, S.; Marder, S. R.; Hardcastle, K. I.; Bunz, U. H. F. *Synlett* **2011**, *2011*, 1983−1986.
(105) Goetz, K. P.; Li, Z.; Ward, J. W.; Bougher, C.; Rivnay, J.; Smith, J.; Conrad, B. R.; Parkin, S. R.; Anthopoulos, T. D.; Salleo, A.; Anthony, J. E.; Jurchescu, O. D. *Adv. Mater.* **2011**, *23*, 3698−3703.
(106) Verlaak, S.; Steudel, S.; Heremans, P.; Janssen, D.; Deleuze, M. S. *Phys. Rev. B* **2003**, *68*, 195409.
(107) Liu, Y.; Wang, Y.; Wu, W.; Liu, Y.; Xi, H.; Wang, L.; Qiu, W.; Lu, K.; Du, C.; Yu, G. *Adv. Funct. Mater.* **2009**, *19*, 772−778.
(108) Xiao, K.; Liu, Y.; Qi, T.; Zhang, W.; Wang, F.; Gao, J.; Qiu, W.; Ma, Y.; Cui, G.; Chen, S.; Zhan, X.; Yu, G.; Qin, J.; Hu, W.; Zhu, D. *J. Am. Chem. Soc.* **2005**, *127*, 13281−13286.
(109) Liu, Y.; Sun, X.; Di, C.-a.; Liu, Y.; Du, C.; Lu, K.; Ye, S.; Yu, G. *Chem. Asian J.* **2010**, *5*, 1550−1554.
(110) Zhang, X.; Côté, A. P.; Matzger, A. J. *J. Am. Chem. Soc.* **2005**, *127*, 10502−10503.
(111) Okamoto, T.; Kudoh, K.; Wakamiya, A.; Yamaguchi, S. *Chem.—Eur. J.* **2007**, *13*, 548−556.
(112) Niimi, K.; Shinamura, S.; Osaka, I.; Miyazaki, E.; Takimiya, K. *J. Am. Chem. Soc.* **2011**, *133*, 8732−8739.
(113) Tang, M. L.; Okamoto, T.; Bao, Z. *J. Am. Chem. Soc.* **2006**, *128*, 16002−16003.
(114) Tang, M. L.; Mannsfeld, S. C. B.; Sun, Y.-S.; Becerril, H. c. A.; Bao, Z. *J. Am. Chem. Soc.* **2009**, *131*, 882−883.
(115) Laquindanum, J. G.; Katz, H. E.; Lovinger, A. J. *J. Am. Chem. Soc.* **1998**, *120*, 664−672.
(116) Pho, T. V.; Yuen, J. D.; Kurzman, J. A.; Smith, B. G.; Miao, M.; Walker, W. T.; Seshadri, R.; Wudl, F. *J. Am. Chem. Soc.* **2012**, *134*, 18185−18188.
(117) Yamada, K.; Okamoto, T.; Kudoh, K.; Wakamiya, A.; Yamaguchi, S.; Takeya, J. *Appl. Phys. Lett.* **2007**, *90*, 072102.
(118) Okamoto, T.; Kudoh, K.; Wakamiya, A.; Yamaguchi, S. *Org. Lett.* **2005**, *7*, 5301−5304.
(119) Kunugi, Y.; Takimiya, K.; Yamane, K.; Yamashita, K.; Aso, Y.; Otsubo, T. *Chem. Mater.* **2002**, *15*, 6−7.
(120) Takimiya, K.; Kunugi, Y.; Konda, Y.; Niihara, N.; Otsubo, T. *J. Am. Chem. Soc.* **2004**, *126*, 5084−5085.
(121) Yamamoto, T.; Takimiya, K. *J. Am. Chem. Soc.* **2007**, *129*, 2224−2225.
(122) Dadvand, A.; Cicoira, F.; Chernichenko, K. Y.; Balenkova, E. S.; Osuna, R. M.; Rosei, F.; Nenajdenko, V. G.; Perepichka, D. F. *Chem. Commun.* **2008**, 5354−5356.
(123) Nakano, M.; Niimi, K.; Miyazaki, E.; Osaka, I.; Takimiya, K. *J. Org. Chem.* **2012**, *77*, 8099−8111.
(124) Qi, T.; Guo, Y.; Liu, Y.; Xi, H.; Zhang, H.; Gao, X.; Liu, Y.; Lu, K.; Du, C.; Yu, G.; Zhu, D. *Chem. Commun.* **2008**, 6227−6229.

(125) Gao, J. H.; Li, R. J.; Li, L. Q.; Meng, Q.; Jiang, H.; Li, H. X.; Hu, W. P. *Adv. Mater.* **2007**, *19*, 3008−3011.
(126) Li, R.; Dong, H.; Zhan, X.; He, Y.; Li, H.; Hu, W. *J. Mater. Chem.* **2010**, *20*, 6014−6018.
(127) Zhao, H.; Jiang, L.; Dong, H.; Li, H.; Hu, W.; Ong, B. S. *ChemPhysChem* **2009**, *10*, 2345−2348.
(128) Bao, Z.; Lovinger, A. J.; Dodabalapur, A. *Adv. Mater.* **1997**, *9*, 42−44.
(129) Shea, P. B.; Kanicki, J.; Ono, N. *J. Appl. Phys.* **2005**, *98*, 014503.
(130) Shea, P. B.; Pattison, L. R.; Kawano, M.; Chen, C.; Chen, J.; Petroff, P.; Martin, D. C.; Yamada, H.; Ono, N.; Kanicki, J. *Synth. Met.* **2007**, *157*, 190−197.
(131) Tang, Q.; Zhang, D.; Wang, S.; Ke, N.; Xu, J.; Yu, J. C.; Miao, Q. *Chem. Mater.* **2009**, *21*, 1400−1405.
(132) Liang, Z.; Tang, Q.; Mao, R.; Liu, D.; Xu, J.; Miao, Q. *Adv. Mater.* **2011**, *23*, 5514−5518.
(133) Liang, Z.; Tang, Q.; Xu, J.; Miao, Q. *Adv. Mater.* **2011**, *23*, 1535−1539.
(134) Wang, C.; Liang, Z.; Liu, Y.; Wang, X.; Zhao, N.; Miao, Q.; Hu, W.; Xu, J. *J. Mater. Chem.* **2011**, *21*, 15201−15204.
(135) Jones, B. A.; Facchetti, A.; Wasielewski, M. R.; Marks, T. J. *J. Am. Chem. Soc.* **2007**, *129*, 15259−15278.
(136) Newman, C. R.; Frisbie, C. D.; da Silva Filho, D. A.; Brédas, J.-L.; Ewbank, P. C.; Mann, K. R. *Chem. Mater.* **2004**, *16*, 4436−4451.
(137) Bao, Z.; Lovinger, A. J.; Brown, J. *J. Am. Chem. Soc.* **1998**, *120*, 207−208.
(138) Sakamoto, Y.; Suzuki, T.; Kobayashi, M.; Gao, Y.; Fukai, Y.; Inoue, Y.; Sato, F.; Tokito, S. *J. Am. Chem. Soc.* **2004**, *126*, 8138−8140.
(139) Delgado, M. C. R.; Pigg, K. R.; da Silva Filho, D. t. A.; Gruhn, N. E.; Sakamoto, Y.; Suzuki, T.; Osuna, R. M.; Casado, J.; Hernández, V. c.; Navarrete, J. T. L. p.; Martinelli, N. G.; Cornil, J.; Sánchez-Carrera, R. S.; Coropceanu, V.; Brédas, J.-L. *J. Am. Chem. Soc.* **2009**, *131*, 1502−1512.
(140) Tang, M. L.; Reichardt, A. D.; Siegrist, T.; Mannsfeld, S. C. B.; Bao, Z. *Chem. Mater.* **2008**, *20*, 4669−4676.
(141) Tang, M. L.; Reichardt, A. D.; Miyaki, N.; Stoltenberg, R. M.; Bao, Z. *J. Am. Chem. Soc.* **2008**, *130*, 6064−6065.
(142) Tang, M. L.; Oh, J. H.; Reichardt, A. D.; Bao, Z. *J. Am. Chem. Soc.* **2009**, *131*, 3733−3740.
(143) Tang, M. L.; Bao, Z. *Chem. Mater.* **2010**, *23*, 446−455.
(144) Moon, H.; Zeis, R.; Borkent, E.-J.; Besnard, C.; Lovinger, A. J.; Siegrist, T.; Kloc, C.; Bao, Z. *J. Am. Chem. Soc.* **2004**, *126*, 15322−15323.
(145) Chi, X.; Li, D.; Zhang, H.; Chen, Y.; Garcia, V.; Garcia, C.; Siegrist, T. *Org. Electron.* **2008**, *9*, 234−240.
(146) Yoon, M.-H.; Facchetti, A.; Stern, C. E.; Marks, T. J. *J. Am. Chem. Soc.* **2006**, *128*, 5792−5801.
(147) Gsänger, M.; Oh, J. H.; Könemann, M.; Höffken, H. W.; Krause, A.-M.; Bao, Z.; Würthner, F. *Angew. Chem.* **2010**, *122*, 752−755.
(148) Jones, B. A.; Ahrens, M. J.; Yoon, M.-H.; Facchetti, A.; Marks, T. J.; Wasielewski, M. R. *Angew. Chem., Int. Ed.* **2004**, *43*, 6363−6366.
(149) Mei, J.; Graham, K. R.; Stalder, R.; Tiwari, S. P.; Cheun, H.; Shim, J.; Yoshio, M.; Nuckolls, C.; Kippelen, B.; Castellano, R. K.; Reynolds, J. R. *Chem. Mater.* **2011**, *23*, 2285−2288.
(150) Kanimozhi, C.; Yaacobi-Gross, N.; Chou, K. W.; Amassian, A.; Anthopoulos, T. D.; Patil, S. *J. Am. Chem. Soc.* **2012**, *134*, 16532−16535.
(151) Virkar, A. A.; Mannsfeld, S.; Bao, Z.; Stingelin, N. *Adv. Mater.* **2010**, *22*, 3857−3875.
(152) Babel, A.; Jenekhe, S. A. *Synth. Met.* **2005**, *148*, 169−173.
(153) Anthony, J. E. *Chem. Rev.* **2006**, *106*, 5028−5048.
(154) Anthony, J. E.; Eaton, D. L.; Parkin, S. R. *Org. Lett.* **2001**, *4*, 15−18.
(155) Anthony, J. E.; Brooks, J. S.; Eaton, D. L.; Parkin, S. R. *J. Am. Chem. Soc.* **2001**, *123*, 9482−9483.
(156) Payne, M. M.; Delcamp, J. H.; Parkin, S. R.; Anthony, J. E. *Org. Lett.* **2004**, *6*, 1609−1612.
(157) Lehnherr, D.; Waterloo, A. R.; Goetz, K. P.; Payne, M. M.; Hampel, F.; Anthony, J. E.; Jurchescu, O. D.; Tykwinski, R. R. *Org. Lett.* **2012**, *14*, 3660−3663.
(158) Payne, M. M.; Parkin, S. R.; Anthony, J. E. *J. Am. Chem. Soc.* **2005**, *127*, 8028−8029.
(159) Kang, M. J.; Yamamoto, T.; Shinamura, S.; Miyazaki, E.; Takimiya, K. *Chem. Sci.* **2010**, *1*, 179−183.
(160) Reese, C.; Roberts, M. E.; Parkin, S. R.; Bao, Z. *Adv. Mater.* **2009**, *21*, 3678−3681.
(161) Yuan, Q.; Mannsfeld, S. C. B.; Tang, M. L.; Roberts, M.; Toney, M. F.; DeLongchamp, D. M.; Bao, Z. *Chem. Mater.* **2008**, *20*, 2763−2772.
(162) Shin, T. J.; Yang, H.; Ling, M.-m.; Locklin, J.; Yang, L.; Lee, B.; Roberts, M. E.; Mallik, A. B.; Bao, Z. *Chem. Mater.* **2007**, *19*, 5882−5889.
(163) Stoliar, P.; Kshirsagar, R.; Massi, M.; Annibale, P.; Albonetti, C.; de Leeuw, D. M.; Biscarini, F. *J. Am. Chem. Soc.* **2007**, *129*, 6477−6484.
(164) Wei, Z.; Hong, W.; Geng, H.; Wang, C.; Liu, Y.; Li, R.; Xu, W.; Shuai, Z.; Hu, W.; Wang, Q.; Zhu, D. *Adv. Mater.* **2010**, *22*, 2458−2462.
(165) Głowacki, E. D.; Irimia-Vladu, M.; Kaltenbrunner, M.; Gąsiorowski, J.; White, M. S.; Monkowius, U.; Romanazzi, G.; Suranna, G. P.; Mastrorilli, P.; Sekitani, T.; Bauer, S.; Someya, T.; Torsi, L.; Sariciftci, N. S. *Adv. Mater.* **2012**, *25*, 1563−1569.
(166) Irimia-Vladu, M.; Głowacki, E. D.; Troshin, P. A.; Schwabegger, G.; Leonat, L.; Susarova, D. K.; Krystal, O.; Ullah, M.; Kanbur, Y.; Bodea, M. A.; Razumov, V. F.; Sitter, H.; Bauer, S.; Sariciftci, N. S. *Adv. Mater.* **2012**, *24*, 375−380.
(167) He, Z.; Liu, D.; Mao, R.; Tang, Q.; Miao, Q. *Org. Lett.* **2012**, *14*, 1050−1053.
(168) Feng, X.; Marcon, V.; Pisula, W.; Hansen, M. R.; Kirkpatrick, J.; Grozema, F.; Andrienko, D.; Kremer, K.; Muellen, K. *Nat. Mater.* **2009**, *8*, 421−426.
(169) Li, W.-S.; Yamamoto, Y.; Fukushima, T.; Saeki, A.; Seki, S.; Tagawa, S.; Masunaga, H.; Sasaki, S.; Takata, M.; Aida, T. *J. Am. Chem. Soc.* **2008**, *130*, 8886−8887.
(170) Okamoto, T.; Nakahara, K.; Saeki, A.; Seki, S.; Oh, J. H.; Akkerman, H. B.; Bao, Z.; Matsuo, Y. *Chem. Mater.* **2011**, *23*, 1646−1649.
(171) Katz, H. E.; Lovinger, A. J.; Johnson, J.; Kloc, C.; Siegrist, T.; Li, W.; Lin, Y. Y.; Dodabalapur, A. *Nature* **2000**, *404*, 478−481.
(172) Chang, P. C.; Lee, J.; Huang, D.; Subramanian, V.; Murphy, A. R.; Fréchet, J. M. J. *Chem. Mater.* **2004**, *16*, 4783−4789.
(173) DeLongchamp, D. M.; Jung, Y.; Fischer, D. A.; Lin, E. K.; Chang, P.; Subramanian, V.; Murphy, A. R.; Fréchet, J. M. J. *J. Phys. Chem. B* **2006**, *110*, 10645−10650.
(174) Murphy, A. R.; Chang, P. C.; VanDyke, P.; Liu, J.; Fréchet, J. M. J.; Subramanian, V.; DeLongchamp, D. M.; Sambasivan, S.; Fischer, D. A.; Lin, E. K. *Chem. Mater.* **2005**, *17*, 6033−6041.
(175) Mauldin, C. E.; Puntambekar, K.; Murphy, A. R.; Liao, F.; Subramanian, V.; Fréchet, J. M. J.; DeLongchamp, D. M.; Fischer, D. A.; Toney, M. F. *Chem. Mater.* **2009**, *21*, 1927−1938.
(176) Oh, J. H.; Lee, W.-Y.; Noe, T.; Chen, W.-C.; Könemann, M.; Bao, Z. *J. Am. Chem. Soc.* **2011**, *133*, 4204−4207.
(177) Locklin, J.; Li, D.; Mannsfeld, S. C. B.; Borkent, E.-J.; Meng, H.; Advincula, R.; Bao, Z. *Chem. Mater.* **2005**, *17*, 3366−3374.
(178) Shukla, D.; Nelson, S. F.; Freeman, D. C.; Rajeswaran, M.; Ahearn, W. G.; Meyer, D. M.; Carey, J. T. *Chem. Mater.* **2008**, *20*, 7486−7491.
(179) Mei, J.; Graham, K. R.; Stalder, R.; Reynolds, J. R. *Org. Lett.* **2010**, *12*, 660−663.
(180) Yang, L.; Tumbleston, J. R.; Zhou, H.; Ade, H.; You, W. *Energy Environ. Sci.* **2013**, *6*, 316−326.
(181) Liang, Y.; Feng, D.; Wu, Y.; Tsai, S.-T.; Li, G.; Ray, C.; Yu, L. *J. Am. Chem. Soc.* **2009**, *131*, 7792−7799.
(182) Hou, J.; Chen, H.-Y.; Zhang, S.; Chen, R. I.; Yang, Y.; Wu, Y.; Li, G. *J. Am. Chem. Soc.* **2009**, *131*, 15586−15587.

(183) Price, S. C.; Stuart, A. C.; Yang, L.; Zhou, H.; You, W. *J. Am. Chem. Soc.* **2011**, *133*, 4625−4631.
(184) Zhou, H.; Yang, L.; Stuart, A. C.; Price, S. C.; Liu, S.; You, W. *Angew. Chem., Int. Ed.* **2011**, *50*, 2995−2998.
(185) Shi, Q.; Fan, H.; Liu, Y.; Chen, J.; Ma, L.; Hu, W.; Shuai, Z.; Li, Y.; Zhan, X. *Macromolecules* **2011**, *44*, 4230−4240.
(186) Ko, S.; Verploegen, E.; Hong, S.; Mondal, R.; Hoke, E. T.; Toney, M. F.; McGehee, M. D.; Bao, Z. *J. Am. Chem. Soc.* **2011**, *133*, 16722−16725.
(187) Biniek, L.; Fall, S.; Chochos, C. L.; Anokhin, D. V.; Ivanov, D. A.; Leclerc, N.; Lévêque, P.; Heiser, T. *Macromolecules* **2010**, *43*, 9779−9786.
(188) Cho, S.; Seo, J. H.; Kim, S. H.; Song, S.; Jin, Y.; Lee, K.; Suh, H.; Heeger, A. J. *Appl. Phys. Lett.* **2008**, *93*, 263301.
(189) Bao, Z.; Lovinger, A. J. *Chem. Mater.* **1999**, *11*, 2607−2612.
(190) Li, H.; Mei, J.; Ayzner, A. L.; Toney, M. F.; Tok, J. B. H.; Bao, Z. *Org. Electron.* **2012**, *13*, 2450−2460.
(191) Lee, J.; Han, A. R.; Kim, J.; Kim, Y.; Oh, J. H.; Yang, C. *J. Am. Chem. Soc.* **2012**, *134*, 20713−20721.
(192) Nguyen, T.-Q.; Wu, J.; Doan, V.; Schwartz, B. J.; Tolbert, S. H. *Science* **2000**, *288*, 652−656.
(193) Deng, Y.; Chen, Y.; Zhang, X.; Tian, H.; Bao, C.; Yan, D.; Geng, Y.; Wang, F. *Macromolecules* **2012**, *45*, 8621−8627.
(194) Zhang, W.; Smith, J.; Watkins, S. E.; Gysel, R.; McGehee, M.; Salleo, A.; Kirkpatrick, J.; Ashraf, S.; Anthopoulos, T.; Heeney, M.; McCulloch, I. *J. Am. Chem. Soc.* **2010**, *132*, 11437−11439.
(195) Becerril, H. A.; Miyaki, N.; Tang, M. L.; Mondal, R.; Sun, Y.-S.; Mayer, A. C.; Parmer, J. E.; McGehee, M. D.; Bao, Z. *J. Mater. Chem.* **2009**, *19*, 591−593.
(196) Li, Y.; Wu, Y.; Ong, B. S. *Macromolecules* **2006**, *39*, 6521−6527.
(197) Patra, A.; Bendikov, M. *J. Mater. Chem.* **2010**, *20*, 422−433.
(198) Shahid, M.; McCarthy-Ward, T.; Labram, J.; Rossbauer, S.; Domingo, E. B.; Watkins, S. E.; Stingelin, N.; Anthopoulos, T. D.; Heeney, M. *Chem. Sci.* **2012**, *3*, 181−185.
(199) Hamilton, R.; Bailey, C.; Duffy, W.; Heeney, M.; Shkunov, M.; Sparrowe, D.; Tierney, S.; McCulloch, I.; Kline, R. J.; DeLongchamp, D. M.; Chabinyc, M. *Proc. SPIE* **2006**, 633611−633611.
(200) Debije, M. G.; Piris, J.; de Haas, M. P.; Warman, J. M.; Tomović, Ž.; Simpson, C. D.; Watson, M. D.; Müllen, K. *J. Am. Chem. Soc.* **2004**, *126*, 4641−4645.
(201) Islam, M. M.; Valiyev, F.; Lu, H.-F.; Kuo, M.-Y.; Chao, I.; Tao, Y.-T. *Chem. Commun.* **2011**, *47*, 2008−2010.
(202) Ito, S.; Herwig, P. T.; Böhme, T.; Rabe, J. P.; Rettig, W.; Müllen, K. *J. Am. Chem. Soc.* **2000**, *122*, 7698−7706.
(203) Sagade, A. A.; Rao, K. V.; Mogera, U.; George, S. J.; Datta, A.; Kulkarni, G. U. *Adv. Mater.* **2012**, *25*, 559−564.
(204) Diez-Perez, I.; Li, Z.; Hihath, J.; Li, J.; Zhang, C.; Yang, X.; Zang, L.; Dai, Y.; Feng, X.; Muellen, K.; Tao, N. *Nat Commun* **2010**, *1*, 31.
(205) Hoang, M. H.; Cho, M. J.; Kim, K. H.; Cho, M. Y.; Joo, J.-s.; Choi, D. H. *Thin Solid Films* **2009**, *518*, 501−506.
(206) Senthilkumar, K.; Grozema, F. C.; Bickelhaupt, F. M.; Siebbeles, L. D. A. *J. Chem. Phys.* **2003**, *119*, 9809−9817.
(207) Zhang, Y.; Hanifi, D.; Alvarez, S.; Antonio, F.; Pun, A.; Klivansky, L. M.; Hexemer, A.; Ma, B.; Liu, Y. *Org. Lett.* **2011**, *13*, 6528−6531.
(208) Bouvet, M. *Anal. Bioanal. Chem.* **2006**, *384*, 366−373.
(209) Locklin, J.; Shinbo, K.; Onishi, K.; Kaneko, F.; Bao, Z.; Advincula, R. C. *Chem. Mater.* **2003**, *15*, 1404−1412.
(210) Dong, S.; Bao, C.; Tian, H.; Yan, D.; Geng, Y.; Wang, F. *Adv. Mater.* **2012**, *26*, 1165−1169.
(211) Lv, A.; Puniredd, S. R.; Zhang, J.; Li, Z.; Zhu, H.; Jiang, W.; Dong, H.; He, Y.; Jiang, L.; Li, Y.; Pisula, W.; Meng, Q.; Hu, W.; Wang, Z. *Adv. Mater.* **2012**, *24*, 2626−2630.
(212) Yue, W.; Lv, A.; Gao, J.; Jiang, W.; Hao, L.; Li, C.; Li, Y.; Polander, L. E.; Barlow, S.; Hu, W.; Di Motta, S.; Negri, F.; Marder, S. R.; Wang, Z. *J. Am. Chem. Soc.* **2012**, *134*, 5770−5773.
(213) Schwab, M. G.; Narita, A.; Hernandez, Y.; Balandina, T.; Mali, K. S.; De Feyter, S.; Feng, X.; Müllen, K. *J. Am. Chem. Soc.* **2012**, *134*, 18169−18172.
(214) Genereux, J. C.; Barton, J. K. *Chem. Rev.* **2009**, *110*, 1642−1662.
(215) Slinker, J. D.; Muren, N. B.; Renfrew, S. E.; Barton, J. K. *Nat. Chem.* **2011**, *3*, 228−233.
(216) Sontz, P. A.; Muren, N. B.; Barton, J. K. *Acc. Chem. Res.* **2012**, *45*, 1792−1800.
(217) Ding, X.; Chen, L.; Honsho, Y.; Feng, X.; Saenpawang, O.; Guo, J.; Saeki, A.; Seki, S.; Irle, S.; Nagase, S.; Parasuk, V.; Jiang, D. *J. Am. Chem. Soc.* **2011**, *133*, 14510−14513.
(218) Ding, X.; Guo, J.; Feng, X.; Honsho, Y.; Guo, J.; Seki, S.; Maitarad, P.; Saeki, A.; Nagase, S.; Jiang, D. *Angew. Chem., Int. Ed.* **2011**, *50*, 1289−1293.
(219) Wan, S.; Gandara, F.; Asano, A.; Furukawa, H.; Saeki, A.; Dey, S. K.; Liao, L.; Ambrogio, M. W.; Botros, Y. Y.; Duan, X.; Seki, S.; Stoddart, J. F.; Yaghi, O. M. *Chem. Mater.* **2011**, *23*, 4094−4097.
(220) Finlayson, C. E.; Friend, R. H.; Otten, M. B. J.; Schwartz, E.; Cornelissen, J.; Nolte, R. L. M.; Rowan, A. E.; Samori, P.; Palermo, V.; Liscio, A.; Peneva, K.; Mullen, K.; Trapani, S.; Beljonne, D. *Adv. Funct. Mater.* **2008**, *18*, 3947−3955.
(221) Shklyarevskiy, I. O.; Jonkheijm, P.; Stutzmann, N.; Wasserberg, D.; Wondergem, H. J.; Christianen, P. C. M.; Schenning, A. P. H. J.; de Leeuw, D. M.; Tomović, Ž.; Wu, J.; Müllen, K.; Maan, J. C. *J. Am. Chem. Soc.* **2005**, *127*, 16233−16237.
(222) Dong, S.; Tian, H.; Huang, L.; Zhang, J.; Yan, D.; Geng, Y.; Wang, F. *Adv. Mater.* **2011**, *23*, 2850−2854.
(223) Sergeyev, S.; Pisula, W.; Geerts, Y. H. *Chem. Soc. Rev.* **2007**, *36*, 1902−1929.
(224) Hoofman, R. J. O. M.; de Haas, M. P.; Siebbeles, L. D. A.; Warman, J. M. *Nature* **1998**, *392*, 54−56.
(225) Warman, J. M.; de Haas, M. P.; Dicker, G.; Grozema, F. C.; Piris, J.; Debije, M. G. *Chem. Mater.* **2004**, *16*, 4600−4609.
(226) Lee, J. K.; Jäckel, F.; Moerner, W. E.; Bao, Z. *Small* **2009**, *5*, 2418−2423.
(227) Xu, B.; Tao, N. J. *Science* **2003**, *301*, 1221−1223.
(228) Venkataraman, L.; Klare, J. E.; Nuckolls, C.; Hybertsen, M. S.; Steigerwald, M. L. *Nature* **2006**, *442*, 904−907.
(229) Tour, J. M.; Reinerth, W. A.; Jones, L.; Burgin, T. P.; Zhou, C.-W.; Muller, C. J.; Deshpande, M. R.; Reed, M. A. *Ann. N.Y. Acad. Sci.* **1998**, *852*, 197−204.
(230) Nitzan, A.; Ratner, M. A. *Science* **2003**, *300*, 1384−1389.
(231) Lindsay, S. M.; Ratner, M. A. *Adv. Mater.* **2007**, *19*, 23−31.
(232) Joachim, C.; Ratner, M. A. *Proc. Natl. Acad. Sci. U.S.A.* **2005**, *102*, 8801−8808.
(233) Wold, D. J.; Frisbie, C. D. *J. Am. Chem. Soc.* **2001**, *123*, 5549−5556.
(234) Kline, R. J.; McGehee, M. D.; Kadnikova, E. N.; Liu, J.; Fréchet, J. M. J. *Adv. Mater.* **2003**, *15*, 1519−1522.
(235) Brinkmann, M.; Rannou, P. *Macromolecules* **2009**, *42*, 1125−1130.
(236) Kline, R. J.; McGehee, M. D.; Kadnikova, E. N.; Liu, J.; Fréchet, J. M. J.; Toney, M. F. *Macromolecules* **2005**, *38*, 3312−3319.
(237) Kline, R.; McGehee, M. *J. Macromol. Sci., Polym. Rev.* **2006**, *46*, 27−45.
(238) Sirringhaus, H.; Wilson, R. J.; Friend, R. H.; Inbasekaran, M.; Wu, W.; Woo, E. P.; Grell, M.; Bradley, D. D. C. *Appl. Phy. Lett.* **2000**, *77*, 406−408.
(239) Kas, O. Y.; Charati, M. B.; Rothberg, L. J.; Galvin, M. E.; Kiick, K. L. *J. Mater. Chem.* **2008**, *18*, 3847−3854.
(240) Chou, C.-M.; Lee, S.-L.; Chen, C.-H.; Biju, A. T.; Wang, H.-W.; Wu, Y.-L.; Zhang, G.-F.; Yang, K.-W.; Lim, T.-S.; Huang, M.-J.; Tsai, P.-Y.; Lin, K.-C.; Huang, S.-L.; Chen, C.-h.; Luh, T.-Y. *J. Am. Chem. Soc.* **2009**, *131*, 12579−12585.
(241) Zheng, Y.; Cui, J.; Zheng, J.; Wan, X. *J. Mater. Chem.* **2010**, *20*, 5915−5922.

(242) de Witte, P. A. J.; Castriciano, M.; Cornelissen, J. J. L. M.; Monsù Scolaro, L.; Nolte, R. J. M.; Rowan, A. E. *Chem.—Eur. J.* **2003**, *9*, 1775−1781.
(243) Fang, L.; Bao, Z. Unpublished work.
(244) Xia, Y.; Kornfield, J. A.; Grubbs, R. H. *Macromolecules* **2009**, *42*, 3761−3766.
(245) Colson, J. W.; Woll, A. R.; Mukherjee, A.; Levendorf, M. P.; Spitler, E. L.; Shields, V. B.; Spencer, M. G.; Park, J.; Dichtel, W. R. *Science* **2011**, *332*, 228−231.
(246) Anthony, J. E.; Brooks, J. S.; Eaton, D. L.; Parkin, S. R. *J. Am. Chem. Soc.* **2001**, *123*, 9482−9483.
(247) Nakayama, K.; Hirose, Y.; Soeda, J.; Yoshizumi, M.; Uemura, T.; Uno, M.; Li, W.; Kang, M. J.; Yamagishi, M.; Okada, Y.; Miyazaki, E.; Nakazawa, Y.; Nakao, A.; Takimiya, K.; Takeya, J. *Adv. Mater.* **2011**, *23*, 1626−1629.
(248) Lee, S. S.; Kim, C. S.; Gomez, E. D.; Purushothaman, B.; Toney, M. F.; Wang, C.; Hexemer, A.; Anthony, J. E.; Loo, Y.-L. *Adv. Mater.* **2009**, *21*, 3605−3609.
(249) Rivnay, J.; Jimison, L. H.; Northrup, J. E.; Toney, M. F.; Noriega, R.; Lu, S.; Marks, T. J.; Facchetti, A.; Salleo, A. *Nat. Mater.* **2009**, *8*, 952−958.
(250) Ling, M. M.; Bao, Z. N. *Chem. Mater.* **2004**, *16*, 4824−4840.
(251) Krebs, F. C. *Sol. Energ. Mat. Sol. C* **2009**, *93*, 394−412.
(252) da Silva, D. A.; Kim, E. G.; Bredas, J. L. *Adv. Mater.* **2005**, *17*, 1072−1076.
(253) Okamoto, T.; Senatore, M. L.; Ling, M. M.; Mallik, A. B.; Tang, M. L.; Bao, Z. *Adv. Mater.* **2007**, *19*, 3381−3384.
(254) Sokolov, A. N.; Friščić, T.; MacGillivray, L. R. *J. Am. Chem. Soc.* **2006**, *128*, 2806−2807.
(255) Opitz, A.; Ecker, B.; Wagner, J.; Hinderhofer, A.; Schreiber, F.; Manara, J.; Pflaum, J.; Brütting, W. *Org. Electronics* **2009**, *10*, 1259−1267.
(256) Salzmann, I.; Duhm, S.; Heimel, G.; Oehzelt, M.; Kniprath, R.; Johnson, R. L.; Rabe, J. r. P.; Koch, N. *J. Am. Chem. Soc.* **2008**, *130*, 12870−12871.
(257) Vogel, J.-O.; Salzmann, I.; Opitz, R.; Duhm, S.; Nickel, B.; Rabe, J. P.; Koch, N. *J. Phys. Chem. B* **2007**, *111*, 14097−14101.
(258) Wakayama, Y.; de Oteyza, D. G.; Garcia-Lastra, J. M.; Mowbray, D. J. *ACS Nano* **2010**, *5*, 581−589.
(259) Chen, T.; Pan, G.-B.; Yan, H.-J.; Wan, L.-J.; Matsuo, Y.; Nakamura, E. *J. Phys. Chem. C* **2010**, *114*, 3170−3174.
(260) Blunt, M. O.; Russell, J. C.; Gimenez-LopezMaria del, C.; Taleb, N.; Lin, X.; Schröder, M.; Champness, N. R.; Beton, P. H. *Nat. Chem.* **2011**, *3*, 74−78.
(261) Yuan, G.-C.; Lu, Z.; Xu, Z.; Gong, C.; Song, Q.-L.; Zhao, S.-L.; Zhang, F.-J.; Xu, N.; Gan, Y.; Yang, H.-B.; Li, C. M. *Org. Electron.* **2009**, *10*, 1388−1395.
(262) Kim, D. H.; Lee, H. S.; Yang, H.; Yang, L.; Cho, K. *Adv. Funt. Mater.* **2008**, *18*, 1363−1370.
(263) Dhagat, P.; Haverinen, H. M.; Kline, R. J.; Jung, Y.; Fischer, D. A.; DeLongchamp, D. M.; Jabbour, G. E. *Adv. Funt. Mater.* **2009**, *19*, 2365−2372.
(264) Li, H.; Giri, G.; Tok, J. B.-H.; Bao, Z. *MRS Bull.* **2013**, *38* (1), 34−42.
(265) Lee, W. H.; Cho, J. H.; Cho, K. *J. Mater. Chem.* **2010**, *20*, 2549−2561.
(266) Hunter, C. A.; Sanders, J. K. M. *J. Am. Chem. Soc.* **1990**, *112*, 5525−5534.
(267) Mattheus, C. C.; Dros, A. B.; Baas, J.; Meetsma, A.; de Boer, J. L.; Palstra, T. T. M. *Acta Crystallogr., Sect. C: Cryst. Struct. Commun.* **2001**, *57*, 939−941.
(268) Siegrist, T.; Besnard, C.; Haas, S.; Schiltz, M.; Pattison, P.; Chernyshov, D.; Batlogg, B.; Kloc, C. *Adv. Mater.* **2007**, *19*, 2079−2082.
(269) Henn, D. E.; Williams, W. G.; Gibbons, D. J. *J. Appl. Crystallogr.* **1971**, *4*, 256−256.
(270) Jurchescu, O. D.; Mourey, D. A.; Subramanian, S.; Parkin, S. R.; Vogel, B. M.; Anthony, J. E.; Jackson, T. N.; Gundlach, D. J. *Phys. Rev. B* **2009**, *80*, 085201.
(271) Chen, J.; Anthony, J.; Martin, D. C. *J. Phys. Chem. B* **2006**, *110*, 16397−16403.
(272) Yuan, Q.; Mannsfeld, S. C. B.; Tang, M. L.; Toney, M. F.; Luening, J.; Bao, Z. *J. Am. Chem. Soc.* **2008**, *130*, 3502−3508.
(273) Giri, G.; Verploegen, E.; Mannsfeld, S. C. B.; Atahan-Evrenk, S.; Kim, D. H.; Lee, S. Y.; Becerril, H. A.; Aspuru-Guzik, A.; Toney, M. F.; Bao, Z. A. *Nature* **2011**, *480*, 504−U124.
(274) Fox, D.; Labes, M. M.; Weissberger, A.; McCrone, W. C., Eds. Interscience Publishers: London, 1965; Vol. *1962*; pp 1725−1767.
(275) Cheng, H.-L.; Mai, Y.-S.; Chou, W.-Y.; Chang, L.-R.; Liang, X.-W. *Adv. Funt. Mater.* **2007**, *17*, 3639−3649.
(276) Mannsfeld, S. C. B.; Virkar, A.; Reese, C.; Toney, M. F.; Bao, Z. *Adv. Mater.* **2009**, *21*, 2294−2298.
(277) Virkar, A.; Mannsfeld, S.; Oh, J. H.; Toney, M. F.; Tan, Y. H.; Liu, G.-y.; Scott, J. C.; Miller, R.; Bao, Z. *Adv. Funt. Mater.* **2009**, *19*, 1962−1970.
(278) Cheng, H.-L.; Lin, J.-W. *Cryst. Growth Des.* **2010**, *10*, 4501−4508.
(279) Becerril, H. A.; Roberts, M. E.; Liu, Z.; Locklin, J.; Bao, Z. *Adv. Mater.* **2008**, *20*, 2588−2594.
(280) Chen, J.; Tee, C. K.; Shtein, M.; Martin, D. C.; Anthony, J. *Org. Electron.* **2009**, *10*, 696−703.
(281) Lee, W. H.; Kim, D. H.; Jang, Y.; Cho, J. H.; Hwang, M.; Park, Y. D.; Kim, Y. H.; Han, J. I.; Cho, K. *Appl. Phys. Lett.* **2007**, *90*, 132106.
(282) Wedl, B.; Resel, R.; Leising, G.; Kunert, B.; Salzmann, I.; Oehzelt, M.; Koch, N.; Vollmer, A.; Duhm, S.; Werzer, O.; Gbabode, G.; Sferrazza, M.; Geerts, Y. *RSC Adv.* **2012**, *2*, 4404−4414.
(283) Amassian, A.; Pozdin, V. A.; Li, R. P.; Smilgies, D. M.; Malliaras, G. G. *J. Mater. Chem.* **2010**, *20*, 2623−2629.
(284) Smilgies, D.-M.; Li, R.; Giri, G.; Chou, K. W.; Diao, Y.; Bao, Z.; Amassian, A. *Phys. Status Solidi RRL* **2013**, *7*, 177−179.
(285) Verploegen, E.; Mondal, R.; Bettinger, C. J.; Sok, S.; Toney, M. F.; Bao, Z. A. *Adv. Funt. Mater.* **2010**, *20*, 3519−3529.
(286) Bottiger, A. P. L.; Jorgensen, M.; Menzel, A.; Krebs, F. C.; Andreasen, J. W. *J. Mater. Chem.* **2012**, *22*, 22501−22509.
(287) Clancy, P. *Chem. Mater.* **2011**, *23*, 522−543.
(288) Liu, S. H.; Wang, W. C. M.; Briseno, A. L.; Mannsfeld, S. C. B.; Bao, Z. *Adv. Mater.* **2009**, *21*, 1217−1232.
(289) Briseno, A. L.; Aizenberg, J.; Han, Y.-J.; Penkala, R. A.; Moon, H.; Lovinger, A. J.; Kloc, C.; Bao, Z. *J. Am. Chem. Soc.* **2005**, *127*, 12164−12165.
(290) Liu, S.; Briseno, A. L.; Mannsfeld, S. C. B.; You, W.; Locklin, J.; Lee, H. W.; Xia, Y.; Bao, Z. *Adv. Funt. Mater.* **2007**, *17*, 2891−2896.
(291) Mannsfeld, S. C. B.; Briseno, A. L.; Liu, S.; Reese, C.; Roberts, M. E.; Bao, Z. *Adv. Funt. Mater.* **2007**, *17*, 3545−3553.
(292) Kloc, C.; Simpkins, P. G.; Siegrist, T.; Laudise, R. A. *J. Cryst. Growth* **1997**, *182*, 416−427.
(293) Laudise, R. A.; Kloc, C.; Simpkins, P. G.; Siegrist, T. *J. Cryst. Growth* **1998**, *187*, 449−454.
(294) Podzorov, V.; Pudalov, V. M.; Gershenson, M. E. *Appl. Phys. Lett.* **2003**, *82*, 1739−1741.
(295) Kim, D. H.; Lee, D. Y.; Lee, H. S.; Lee, W. H.; Kim, Y. H.; Han, J. I.; Cho, K. *Adv. Mater.* **2007**, *19*, 678−682.
(296) Liu, C.; Minari, T.; Lu, X.; Kumatani, A.; Takimiya, K.; Tsukagoshi, K. *Adv. Mater.* **2011**, *23*, 523−526.
(297) Lei, T.; Pei, J. *J. Mater. Chem.* **2012**, *22*, 785−798.
(298) Liu, N.; Zhou, Y.; Ai, N.; Luo, C.; Peng, J.; Wang, J.; Pei, J.; Cao, Y. *Langmuir* **2011**, *27*, 14710−14715.
(299) Jiang, W.; Zhou, Y.; Geng, H.; Jiang, S.; Yan, S.; Hu, W.; Wang, Z.; Shuai, Z.; Pei, J. *J. Am. Chem. Soc.* **2010**, *133*, 1−3.
(300) Liu, S.; Wang, W. M.; Briseno, A. L.; Mannsfeld, S. C. E.; Bao, Z. *Adv. Mater.* **2009**, *21*, 1217−1232.
(301) Day, G. M.; Cooper, T. G.; Cruz-Cabeza, A. J.; Hejczyk, K. E.; Ammon, H. L.; Boerrigter, S. X. M.; Tan, J. S.; Della Valle, R. G.; Venuti, E.; Jose, J.; Gadre, S. R.; Desiraju, G. R.; Thakur, T. S.; van Eijck, B. P.; Facelli, J. C.; Bazterra, V. E.; Ferraro, M. B.; Hofmann, D. W. M.; Neumann, M. A.; Leusen, F. J. J.; Kendrick, J.; Price, S. L.; Misquitta, A. J.; Karamertzanis, P. G.; Welch, G. W. A.; Scheraga, H.

A.; Arnautova, Y. A.; Schmidt, M. U.; van de Streek, J.; Wolf, A. K.; Schweizer, B. *Acta Crystallogr., Sect. B: Struct. Sci.* **2009**, *65*, 107−125.
(302) Beran, G. J. O.; Nanda, K. *J. Phys. Chem. Lett.* **2010**, *1*, 3480−3487.
(303) Yamamoto, T.; Takimiya, K. *J. Photopolym. Sci. Technol.* **2007**, *20*, 57−59.